ANALYSIS OF TRU-FUELED VHTR PRISMATIC CORE PERFORMANCE DOMAINS

A Thesis

by

TOM GOSLEE LEWIS, III

Submitted to the Office of Graduate Studies of
Texas A&M University
in partial fulfillment of the requirements for the degree of

MASTER OF SCIENCE

December 2007

Major Subject: Nuclear Engineering

ANALYSIS OF TRU-FUELED VHTR PRISMATIC CORE PERFORMANCE DOMAINS

A Thesis

by

TOM GOSLEE LEWIS, III

Submitted to the Office of Graduate Studies of
Texas A&M University
in partial fulfillment of the requirements for the degree of

MASTER OF SCIENCE

Approved by:

Chair of Committee,	Pavel Tsvetkov
Committee Members,	William S. Charlton
	Guergana Petrova
	John W. Poston Sr.
Head of Department,	Raymond Juzaitis

December 2007

Major Subject: Nuclear Engineering

ABSTRACT

Analysis of TRU-Fueled VHTR Prismatic Core

Performance Domains. (December 2007)

Tom Goslee Lewis, III, B.S., Texas A&M University

Chair of Advisory Committee: Dr. Pavel Tsvetkov

The current waste management strategy for spent nuclear fuel (SNF) mandated by the U.S. Congress is the disposal of high-level waste (HLW) in a geological repository at Yucca Mountain. Ongoing efforts on closed-fuel cycle options and difficulties in opening and safeguarding such a repository have led to investigations of alternative waste management strategies. One potential strategy would make use of fuels containing transuranic (TRU) nuclides in nuclear reactors. This would prolong reactor operation on a single fuel loading and by doing so, would reduce current HLW stockpiles. The analysis has already shown that high-temperature gas-cooled reactors (HTGRs) and their Generation IV extensions, very-high-temperature reactors (VHTRs), have encouraging performance characteristics that will allow for prolonged operation with no intermediate refueling, as well as for transmutation of TRUs.

The objective of this research was to show that TRU-fueled VHTRs have the possibility of prolonged operation on a single fuel loading while retaining their Generation IV safety features. In addition, this research evaluated performance characteristics, and identified operational domains of these systems, as well as the possibility of HLW reduction.

A whole-core, 3-D model of a power size prismatic VHTR with a detailed temperature distribution was developed for calculations with the SCALE 5.1 code package. Results of extensive criticality and depletion calculations with multiple fuel loadings showed that VHTRs are capable and suitable for autonomous operation when loaded with TRU fuel.

DEDICATION

I would like to dedicate this work to those who helped me with both my research and outside my research.

Especially I thank my parents and sister who have always been available for support.

My advisor, Dr. Pavel Tsvetkov, for always pushing me to find my own solutions and for guidance through this research process.

ACKNOWLEDGEMENTS

I would like to express my full gratitude to all those who gave me the possibility to complete this thesis. I am deeply indebted to my advisor Dr. Tsvetkov, whose broad knowledge, stimulating suggestions and encouragement was the leading force behind the research for and writing of this thesis. I also would like to extend my gratitude to my committee members, Dr. Poston, Dr. Charlton, and Dr. Petrova, for without their support and time I would not have met success.

I would also like to thank Dr. Mark DeHart who spent so much personal time answering a never-ending barrage of e-mails and updating the SCALE code package that was so crucial to my research efforts.

The research for this thesis was funded in part by the US Department of Energy under Award Number DE-FC07-05ID14644 (05-094).

NOMENCLATURE

3D	3 Dimensional
AAA	Advanced Accelerator Application
AEI	Advanced Energy Initiative
AFCI	Advanced Fuel Cycle Initiative
AHA	Acetohyroxamic Acid
BOL	Beginning of Life
C/HM	Carbon to Heavy Metal
DOE	Department of Energy
EOL	End of Life
FP	Fission Product
FR	Fast Reactor
GEN IV	Generation IV
GFR	Gas-Cooled Fast Reactor
GIF	Generation-IV International Forum
GNEP	Global Nuclear Energy Partnership
GWd/tHM	gigawatt day per ton of heavy metal
HLW	High-Level Waste
HTGR	High-Temperature Gas-cooled Reactor
HTTR	High-Temperature Test Reactor
LEU	Low-Enriched Uranium

LFR	Lead-Cooled Fast Reactor
LWR	Light Water Reactor
MA	Minor Actinide
MSR	Molten Salt Reactor
MT	Metric Ton
MWth	Megawatt Thermal
NRC	Nuclear Regulatory Commission
ORNL	Oak Ridge National Laboratory
P&T	Partitioning and Transmutation
PUREX	Plutonium Uranium Reduction and Oxidation
PWR	Pressurized Water Reactor
RGPu	Reactor Grade Plutonium
SCWCR	Super-critical Water Cooled Reactor
SFR	Sodium-Cooled Fast Reactor
SNF	Spent Nuclear Fuel
TBP	Tri-Butyl-Phosphate
TRISO	Tristructual Isotropic
TRU	Transuranics
U.S.	United States
UREX	Uranium Extraction
VHTR	Very-High Temperature Reactor

TABLE OF CONTENTS

Page

LIST OF FIGURES

FIGURE Page

FIGURE Page

LIST OF TABLES

TABLE Page

I. INTRODUCTION

It is clear that the past 200 years have seen a leap in humankind's progress, most notably in the medical and engineering fields, which have drastically altered the way humanity interacts with nature. What once was thought impossible has become integrated in the framework of our society and sustains our existence. This is most evident in our capability to release and harvest the energy encapsulated in the very building blocks of nature itself. This statement of course, refers to the advent of nuclear power and its ability to harvest the binding energy of the nucleus. As with the use of any technology, unanticipated obstacles are encountered and lessons are learned that lead the practitioners in an ever-broadening path of knowledge. A path that constantly requires questioning of what was once known and for us to retool the now outdated methods we use to unleash the power of the atom. As humanity has traveled this path, the public has become much more interested in effects of technology on the environment and the constant accelerating need of cleaner and, more importantly, sustainable yet safe energy. There has been a renewed interest in nuclear energy with demands not only for the future but for final solutions of such issues like nuclear waste management.

The U.S. Congress has mandated the disposal of high-level waste (HLW) in a geological repository at Yucca Mountain. With over thirty billion dollars available for the construction and management of the repository, difficulties in opening and safeguarding it have led to investigations of alternative waste management strategies. One potential strategy would make use of reactor fuels containing transuranic (TRU) nuclides in nuclear reactors. For example, to prolong reactor operation on a single fuel loading and, by doing so, to reduce current HLW inventories. Analysis has already shown that high-temperature gas-cooled reactors (HTGRs) and their Generation IV extensions, very-high

---

This thesis follows the style of *Journal of Nuclear Technology*.

temperature reactors (VHTRs), have encouraging performance characteristics that will allow for prolonged operation without intermediate refueling, as well as for transmutation of TRUs [1].

I.A The Fuel Cycle

The first nuclear reactor went critical in 1942 and hove operated commercially since 1956, demonstrating an excellent safety record. Currently there are over 400 nuclear power reactors operating in 31 countries, accounting for about one-fifth of the electrical generation worldwide [2]. In the U.S, commercial reactors operate under a once-through fuel cycle. At the end of this cycle, spent nuclear fuel (SNF) is considered as HLW when it is accepted for permanent disposal. This is due to the Nuclear Regulatory Commission (NRC) defining HLW as either [3]:

1. Spent reactor fuel when it is accepted for disposal.
2. Waste materials remaining after spent fuel is reprocessed.

The current policy in the U.S. is for all HLW from SNF to be placed in the Yucca Mountain geological repository. By law when the waste is emplaced in the mountain, the waste has to be retrievable, which opens the possibility that the mountain can behave, in a sense, as an energy reserve [3]. For this to be true, the U.S. has to undergo a fuel cycle shift, most probably to one of the following three:

1. Partial recycling. In this cycle a portion of the SNF is reprocessed, where a fraction of the actinide material is recovered and fabricated into new fuel, most likely in the form of mixed-oxide (MOX) for thermal reactors.
2. Full fissile recycling. In this scenario all SNF is recovered and reprocessed for the extraction of Pu and U-233 for fuel in both thermal and fast reactors. This process would occur several times until recycling is no longer feasible.
3. Full actinide recycle. In this final scenario, all the SNF would be processed and all the actinides would be used as fuel in fast reactors that would be capable of higher actinide destruction [4].

The removal of low-level waste (LLW) and stable nuclides can reduce the amount of nuclear waste requiring permanent disposal. Waste inventory estimates show that at the time of waste acceptance, there will be more than 70,000 tons of waste located at power reactor sites spread across 39 states [5]. This amount of waste is more then enough to completely fill the geological repository at the capacity mandated by the current U.S. law [6]. Most of this waste is a result of the operation of the U.S. light-water reactor (LWR) fleet (~60% pressurized water reactors [PWR]).

An average PWR produces approximately 30 tons of SNF per year characterized by burnup levels of about 40 GWd/tHM. There are around 11.5 kg/SNF tone of TRUs composed of approximately 10 kg of Plutonium and 1.5 kg of minor actinides (MAs). The remainder consists of fission products (FPs) (~30 kg) and depleted uranium (DU) [7].

Elements labeled as TRUs have atomic numbers greater than 92 (uranium) and are created in nuclear reactors from ^{238}U via neutron capture events and beta minus decays that result in the formation of higher elements. A subset of TRUs, MAs, is composed of Np, Am, and Cm. MAs have very different cross-sections when compared to U and Pu. For example, Np-237 and Am-241 have very large neutron capture cross-sections when compared to U-238. Furthermore, many of Np-237 and Am-241 daughter nuclides have very large fission cross-sections, thus causing the MAs to burn much faster then the U-238 found in LEU fuel [8].

TRUs are the major source of long-term radioactivity in SNF, while FPs are the major contributor to the short-term (500 years) decay heat, radioactivity and local (e.g., water-table and topsoil) toxicity due to their ease of mobility in the environment (e.g., I-129) [9]. If the SNF were to be "partitioned" and "transmutated" (P&T), the resulting fuel waste would require only 1000 years to reach the emission levels of natural uranium [10]. Neutron emission and decay heat of TRUs are shown in Table I [7].

Table I. TRU Neutron Emission and Decay Heat

Nuclide	Half-life (years)	Thermal Fission Cross-section (b)	Total Neutron Emission Assuming Oxide (1/g-s)	Decay Heat (W/g)
Pu-238	87.7	17.9	36000	0.56
Pu-239	2.41E+04	748	96	0.002
Pu-240	6.54E+03	0.06	1300	0.007
Pu-241	14.4	1013	1.23	0.004
Pu-242	3.76E+05	0.0026	2000	0.0001
Np-237	2.14E+06	0.022	0.9	0.00002
Am-241	4.32E+02	3	7000	0.11
Am-243	7.38E+03	0.12	540	0.007
Cm-242	4.46E-01	5.1	2.90E+07	120
Cm-243	2.85E+01	618	1.30E+05	1.7
Cm-244	1.81E+01	1	1.20E+07	2.8
Cf-252	2.65E+00	33	2.35E+12	39

Partitioning is the separation of SNF into desired chemical subsets via either a wet or dry chemical process. This is a crucial step for transmutation to occur, allowing for these chemical subsets to be used in special targets or as a nuclear fuel. Current research efforts in partitioning technology focus on improving these processes and reducing secondary wastes. Additionally, research is being directed toward specific elements, such as curium, due to safety challenges of fuel/target manufacturing [11].

As with all advanced technologies, difficulties exist most notably with the separation of MAs such as Am, Cm, and the lanthanides due to their nearly identical chemical properties. The most widely used industrial partitioning process is called PUREX (Pu U Reduction and Oxidation). PUREX is a wet chemical extraction process based on nitric acid dissolution of the fuel and solvent extraction of U and Pu using tri-butyl-phosphate (TBP). Currently this process is capable of removing both U and Pu at more then 90.0% (up to 99.88%) from SNF, but Am, Cm and other MAs are not removed individually and are simply lumped together with the FPs [12].

The sister process to PUREX is UREX (Uranium Extraction). UREX is a modification of the front end of the PUREX process. It uses the reagent acetohyroxamic acid (AHA) to complex Pu and reduce its valence so that the Pu will remain in the aqueous phase when the uranium is extracted into TBP. This addition to the PUREX process allows for a very high recovery rate of the U from SNF. This also leaves the Pu and TRUs with the minor actinides, and fission products. Such methods are suitable for the retrieval and processing of TRUs as nuclear fuels. UREX is also attractive from the viewpoint of non-proliferation, since Pu and MAs remains in the same waste stream. The Pu would be very difficult to separate from the MAs, making the waste stream less attractive for clandestine weapon programs. There are currently five widely-accepted UREX processes, each in a different stage of development and each with its own promises and drawbacks. These UREX processes differ from one another by the production of different waste streams [13]. The products of each process are shown in Table II.

Table II. UREX Processes

Process	Prod #1	Prod # 2	Prod # 3	Prod # 4	Prod # 5	Prod # 6	Prod # 7
UREX+1	U	Tc	Cs/Sr	TRU+Ln*			
UREX+1a	U	Tc	Cs/Sr	TRU	All FP		
UREX+2	U	Tc	Cs/Sr	Pu+Np	Am+Cm+LN*	FP	
UREX+3	U	Tc	Cs/Sr	Pu+Np	Am+Cm	All FP	
UREX+4	U	Tc	Cs/Sr	Pu+Np	Am	Cm	All FP

**Ln-subgroup of FPs composed of elements in the Lanthanide series.*

Technetium removal is important because of its major long-term contribution to dose levels at a geological repository. Cs and Sr play the major role in the decay heat generation at a repository. Thus, the separation of these nuclides would improve the repository operations and potentially increase its storage capacity. It is important to note that all UREX processes require considerable cooling time of the SNF before partionioning. This is, in part, due to dose limitations for the operation of reprocessing

facilities and radiation damage to chemicals used in these processes. Additional technologies, such as pyro-processing or TRUEX, give the possibility of decreasing the needed cooling time between spent fuel discharge and reprocessing [2].

The expansion of the fuel cycle is crucial for the sustainability of nuclear fuel resources. All current and under construction nuclear power plants operate with uranium as the fuel source. Using only currently identified conventional uranium resources there is approximately 80 years of power production possible assuming no increase in nuclear energy demands or change in how fuel is used (i.e. traditional LWR reactors). If there is a shift to a closed-fuel cycle with fast reactors only, estimates show that without dramatically increasing nuclear power demand, approximately 5000 years could be supported by existing fuel reserves. Though, a switch to fast reactors cannot occur immediately, switching to double-strata fuel cycle, that uses traditional thermal reactors and dedicated fast reactors could sustain current energy demands [16].

Partitioning technologies such as those discussed, are crucial for future fuel cycles that promise the capability to reduce the HLW stockpiles, increase reactor fuel reserves, make possible advanced fuels containing TRU and MA for prolonged life cores, and extend the capacity of the Yucca Mountain repository reducing the need for additional repositories [8]. Partitioning technology is just one step in these future cycles; there is also a need for new reactor designs, advanced transmutation fuels, and global partnerships to assure non-proliferation. These needs are being addressed globally with the founding of several research partnerships.

I.B Generation-IV Reactor Systems

To meet the demand for clean and reliable energy, the Generation-IV International Forum (GIF) was founded in early 2000 to investigate and develop technologies that could be incorporated into the next generation of power reactors. Through this international partnership around 100 different systems were evaluated to meet goals set forth by the forum [17]:

1. Generation IV nuclear energy systems will provide sustainable energy generation that meets clean air objectives and promotes long-term availability of systems and effective fuel utilization for worldwide energy production.
2. Generation IV nuclear energy systems will minimize and manage their nuclear waste and notably reduce the long-term stewardship burden, thereby improving protection for the public health and the environment.
3. Generation IV nuclear energy systems will have a clear life-cycle cost advantage over other energy sources.
4. Generation IV nuclear energy systems will have a level of financial risk comparable to other energy projects.
5. Generation IV nuclear energy systems operations will excel in safety and reliability.
6. Generation IV nuclear energy systems will have a very low likelihood and degree of reactor core damage.
7. Generation IV nuclear energy systems will eliminate the need for offsite emergency response.
8. Generation IV nuclear energy systems will increase the assurance that they are a very unattractive and the least desirable route for diversion or theft of weapons-usable materials, and provide increased physical protection against acts of terrorism.

Of the nearly 100 systems studied by GIF, six were chosen in late 2002 based on the ability of the system to meet the goals outlined above [17]. Three of these systems (the VHTR, super-critical water-cooled reactor (SCWCR), molten salt reactor (MSR)) can operate with a thermal spectrum. The lead-cooled fast reactor (LFR), gas cooled fast reactor (GFR), sodium-cooled fast reactor (SFR), super-critical water-cooled reactor (SCWCR), and molten salt reactor (MSR) can operate as fast reactor systems. Of these six concept systems, the VHTR is the most likely GEN IV system to be available in the near term (~2020) [14].

I.C Very High Temperature Reactors

VHTR technology is based on concepts developed for the U.S. Fort St. Vrain and Peach Bottom reactors [10], as well as on the extensive international experience involving such facilities as the German AVR and THTR, Swiss PROTEUS, Chineese HTR-10, Japanese HTTR and Russian GROG and ASTRA. The VHTR concept should be designed as a high-efficiency system capable of supplying electricity and process heat to a broad spectrum of high-temperature and energy-intensive processes. The reference reactor is a 600 MWth, helium-cooled core connected to an intermediate heat exchanger to deliver process heat, although direct cycles without the need of a heat exchanger have been proposed. The reactor supplies heat with core coolant (helium) outlet temperatures up to 1,000 degrees Celsius [18]. Further VHTR reference operation parameters are shown in Table III.

Table III. VHTR Reference Design

	Reference Value
Reactor power	600 MWth
Coolant inlet/outlet temperature	600/1000 °C
Maximum Fuel Temperature	
Normal Operation	1400 °C
Accident Conditions	1800 °C
Core inlet/outlet pressure	Dependent on process
Coolant	Helium
Core Power Density	5.8 MWth/m^3
Net plant efficiency	>50%
Core Geometry	Annular
Plant Design Life	60 years
Safety Design Philosophy	Passive

The high thermodynamic efficiency of VHTRs is due to their power generation cycle being based on a high-temperature Brayton cycle. The systems are passively safe because of their low-power density and refractory core materials. The low-power density in VHTRs is important in accidents where a loss of cooling requires that energy produced before reactor shutdown, as well as decay heat produced after shutdown can, be dissipated within the reactor by conduction and radiative heat transfer without material failure, specifically the TRISO (TRIstructual ISOtropic)-coated fuel particles. In particular, VHTRs will have several containment layers to minimize the radionuclide release to the environment. These layers include:

1. The fuel kernel,
2. Particle coatings, specifically SiC,
3. Compact/Pebble graphite matrix,
4. Primary coolant pressure boundary, and
5. Vented, low-pressure confinement building,

Of these five containment layers, the most important is the particle coatings. The performance of these coatings during reactor operation is strongly related to the manufacturing process. Currently there are 8 potential failure mechanisms associated with particle failure related to radionuclide release and are listed below [19]:

1. Failure of the SiC coating by thermal decomposition,
2. Failure of the SiC coating by fission product/SiC interaction,
3. Failure of the SiC coating due to kernel migration in the presence of a thermal gradient,
4. Heavy-metal dispersion during SiC coating deposition and subsequent accelerated SiC corrosion during irradiation,
5. Irradiation-induced failure of the OPyC coating,
6. Pressure-induced failure in particles without manufacturing defects,
7. Pressure-induced failure in particles with manufacturing defects, and
8. Coating damage during fuel manufacture, resulting in heavy metal contamination.

VHTRs have a flexible fuel cycle (i.e., cycles not simply based on a once through LEU cycle), allowing for wide range of fuels (e.g., LEU, TRU, reactor grade Pu (RGPu), etc.). The fuel cycle flexibility gives VHTRs the capability to undergo high burnup between refueling, exemplified by the concept of Deep Burn [20].

Deep Burn is a concept proposed and formally patented by General Atomics (GA) for systems such as the modular helium reactor (MHR) that makes use of thermalized neutrons and high-burnup fuel forms for the reduction/destruction of TRUs produced by LWRs. The Deep Burn process is a balance of the fission and neutron-capture-followed-by fission processes that result in a regulated fuel consumption rate [21]. The possibility of such an approach is made possible by the TRISO-coated fuel particles being capable of high burnup (burnup is limited by the molecular structure of a material to withstand radiation damage). To account for radiation damage effects, fuel performance limits are expressed in terms of fast neutron fluence. For of TRISO particles, the fast neutron fluence limits, depending on TRISO configuration, are around 5×10^{25} n/m^2 [19]. The

graphite moderation in a VHTR is also important in the deep burn process, by producing more opportunities for thermal neutrons to interact with fissionable nuclides and epithermal neutrons to interact with non-fissionable nuclides (neutron capture events for transmutation). Neutrons in the epithermal range, when captured, also provide a strong negative reactivity feedback effect as the fuel temperature increases [22]. Additionally, the ceramic-coated fuel particle size can be adjusted, effectively changing the carbon to heavy metal ratio (C/HM), as well as changing self-shielding within the particles, which results in a change in the rate of fission and capture reactions.

There are two possible core types for a VHTR system, the first being a pebble-bed core, such as the Chinese HTR-10, and the second being a prismatic (hexagonal block) core such as the Japanese HTTR [23]. The prismatic core is composed of reflector blocks, fuel blocks, coolant blocks and control rod guide blocks. These blocks are hexagonal graphite blocks that are arranged side-by-side in a honeycomb configuration and then stacked vertically in columns to create the core [10]. This is shown in Fig. 1, which illustrates the two core configurations considered in this thesis.

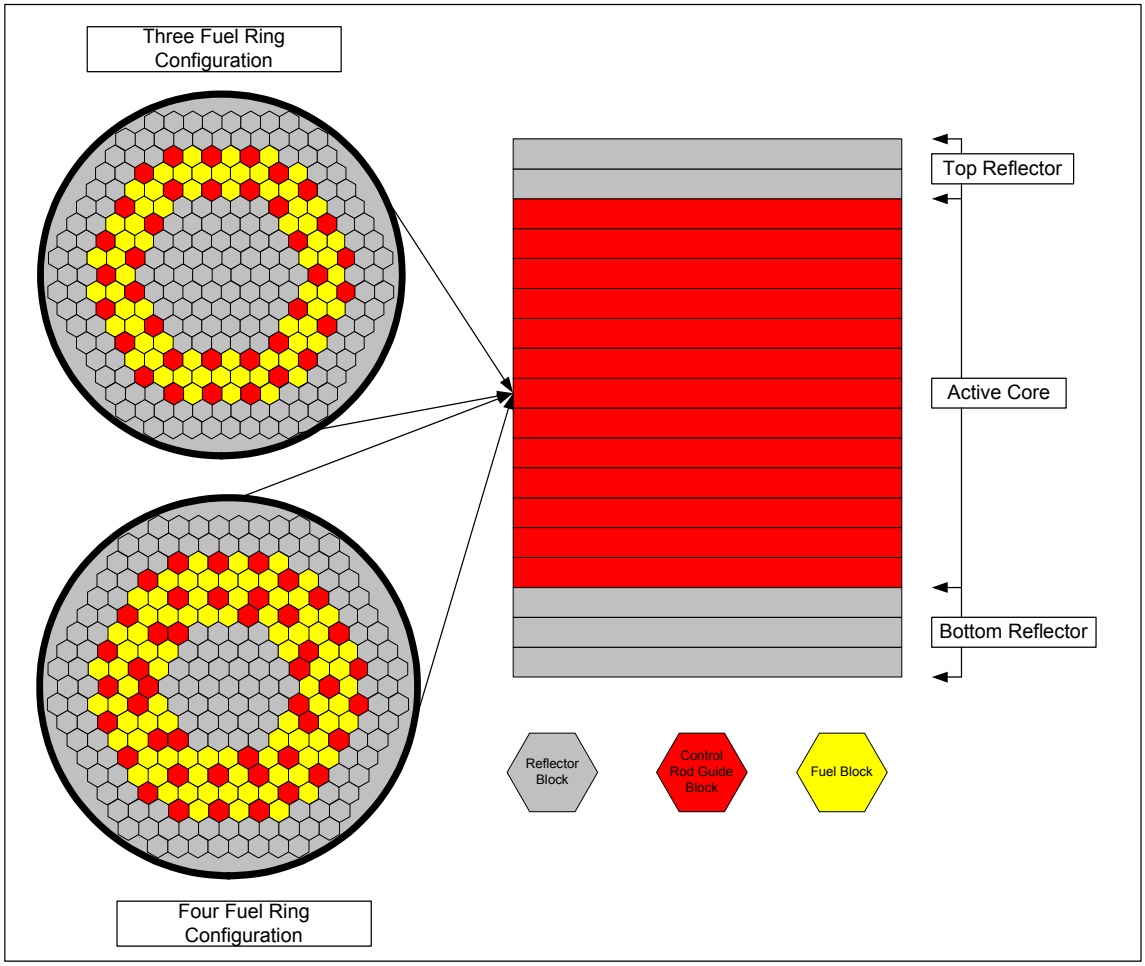

Fig. 1. Three and four fuel-ring VHTR configurations.

The pebble-bed core is composed of a cavity created by graphite reflector blocks that are filled with billiard-ball-sized graphite, spheres containing TRISO-coated fuel particles. Basic features of a TRISO-coated fuel particle are shown in Fig. 2. The TRISO coating on the fuel provides a miniature containment vessel for each fuel particle, allowing retention of fission fragments at high temperatures [14]. The core is cooled with helium that flows through gaps between neighboring graphite spheres. The pebble-bed design has the unique possibility of continuous refueling by the addition and removal of pebbles during reactor operation [10], thus decreasing the need for reactor downtime. Both core

types can achieve similar performance characteristics and both utilize the TRISO-coated fuel particles.

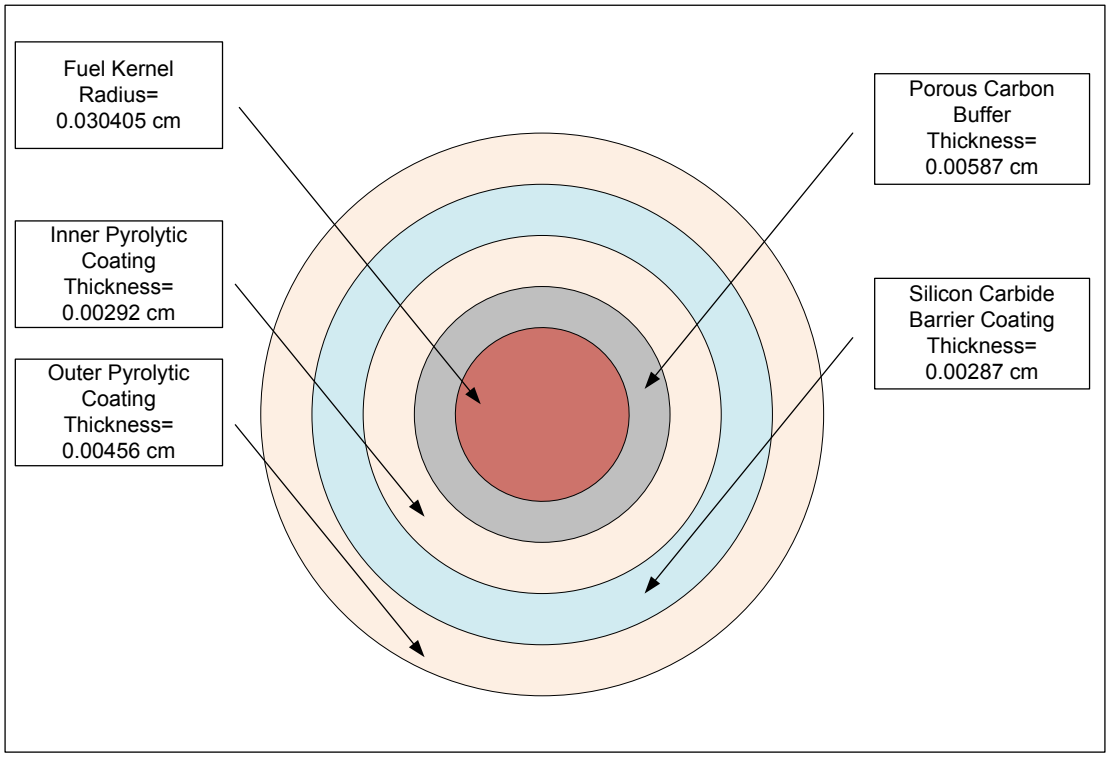

Fig. 2. TRISO-coated fuel particle.

These systems are usually considered to operate under a thermal-neutron spectrum, but have the possibility of their spectrum being shifted to a harder spectrum by changing the fuel-to-moderator ratio. Due to spectrum shifting, there is a possibility to use VHTRs in waste management via incorporating non-traditional fuels that contain different loadings of plutonium, uranium, and MAs [7,8]. The spectrum shifting takes advantage of the more favorable fission cross-sections for nuclides in TRUs at higher energies (i.e., harder spectrum). The utilization of MAs, from light-water reactor (LWR) fuel, for the prolonged-life VHTRs would reduce the need for the creation of more geological

repository volume per decade of reactor operation, if implemented in advanced fuel cycles such as those being developed in the Advanced Fuel Cycle Program [23].

I.D Advanced Fuel Cycle Program

In 2003, the Department of Energy's (DOE) Advanced Fuel Cycle Initiative (AFCI) was launched as an outgrowth of the Congress-authorized Advanced Accelerator Application (AAA) program [24]. The program mission was to "develop and demonstrate technologies that would enable the transition to an environmental, social, economical, and political acceptable advanced fuel cycle [25]". Goals of the program were:

1. Reduce the long-term environmental burden of nuclear energy through more efficient disposal of waste materials,
2. Enhance the overall nuclear fuel cycle proliferation resistance via improved technologies for SNF management,
3. Enhance energy security by extracting energy recoverable from SNF, ensuring that uranium resources do not become a limiting factor for nuclear power, and
4. Improve fuel-cycle management, while continuing competitive fuel-cycle economics and excellent safety performance of the entire fuel-cycle system,

Preliminary analysis of possible AFCI technologies for nuclear waste management options has shown that the cost of a geological repository at the Yucca Mountain site could be reduced by several billion dollars and the need for a second repository could be significantly delayed while increasing the amount of domestic nuclear resources [25]. The increase of domestic nuclear resources is paramount for the sustainability of the industry.

The AFCI program has now been transformed into the Global Nuclear Energy Partnership (GNEP) program, which is the DOE response to President Bush's Advanced Energy Initiative. The GNEP program has similar goals but is more robust by realizing that the nuclear industry is not a domestic entity but rather a global enterprise that assumes contributions from other nations in order to meet future needs. It envisions a

secure, closed, fuel-cycle with supplier nations providing affordable safe reprocessed fuel that can then be transferred to other nations who agree to use nuclear energy for power production as demonstrated in Fig. 3.

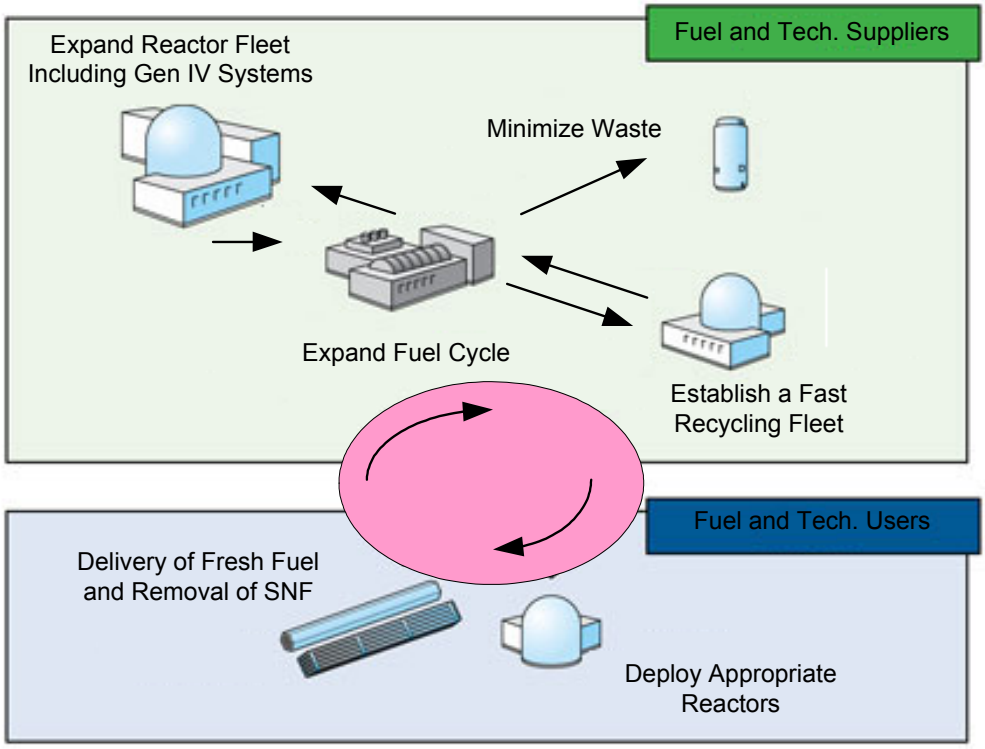

Fig. 3. GNEP fuel cycle concept.

By the creation of the nuclear energy market, as shown in Fig. 3, GNEP aims to accomplish its mission of increasing U.S. and global energy security, reduce the risk of proliferation and improve the environment. Spent Nuclear Fuel (SNF) recycling is paramount to the success of GNEP and is the underlying bond between the AFCI and Gen IV Forum [6, 26].

I.E Research Objectives

The objectives of this research is to analyze TRU-fueled VHTR prismatic core configurations and determine performance domains for VHTRs fueled with TRUs and designed for prolonged operation without intermediate refueling. This overall objective leads to several research targets:

1. Develop a 3D whole-core model representing a power-size VHTR (VHTR capable of 600 MWth+) that accounts for neutronics and thermal characteristics,
2. Develop a 3D temperature distribution that can conceivably be expected in a VHTR configuration and incorporate it into the developed VHTR model,
3. Develop a robust Matlab script that allows automated model generation for use with the SCALE 5.1 code system incorporating the developed temperature distribution and supporting parametric studies,
4. Develop a series of Matlab and Perl scripts facilitating efficient post-processing of simulation results representing VHTR configurations,
5. Analyze basic performance characteristics of the VHTR BOL configurations with LEU, RGPu and TRUs,
6. Analyze performance domains for TRU-fueled VHTRs designed for prolonged operation without intermediate refueling, and
7. Analyze safety and transmutation characteristics of the feasible TRU-fueled VHTR configurations.

Meeting the objectives and research targets of this research is possible because VHTR prismatic core designs have the inherent flexibility of component configuration, fuel utilization, and fuel management. Flexibility in the component configuration allows for the C/HM ratio to be adjusted. C/HM adjustments allow for neutron spectrum shifts, which give the ability to create a harder spectrum in the VHTR core. Harder spectra, in the case of TRU fuels, result in self-stabilization effects extending operation without intermediate refueling.

II. APPLIED COMPUTER CODE SYSTEMS

Fig. 4 shows the code system formed and implemented for studies presented in this research. The neutronics analysis using the 3D, whole-core VHTR model was performed using the ORNL SCALE (Standardized Computer Analysis for Licensing Evaluation) code system. The standard SCALE 5.1 TRITON sequence has been upgraded to allow fuel cycle modeling accounting for double heterogeneity effects. This option was implemented for this project by the ORNL staff (Dr. Mark DeHart) and was not available in the standard distribution package. A combination of Matlab, Excel, and Perl was used to build SCALE input files and analyze SCALE output data as shown in Fig. 4.

II.A SCALE 5.1 Code System

The SCALE code system was being developed and is supported at Oak Ridge National Laboratory (ORNL) under a co-sponsorship of the NRC and DOE. It is a multi-purpose computer code system for the analysis of nuclear facilities and packages including but not limited to reactor physics, fuel cycle, criticality safety, shielding, lattice physics, radiation source terms, SNF and HLW characterization.

The combination, execution and communication between various SCALE functional modules are maintained by control modules. This analysis is based on the capabilities of TRITON and CSAS25 control modules and the corresponding sequences. The SCALE Material Information Processor Library (MIPLIB) allows specifying nuclides, elements, and mixtures based on the Standard Composition Library as well as other keyword and geometry input that is relevant to cross-section processing [27].

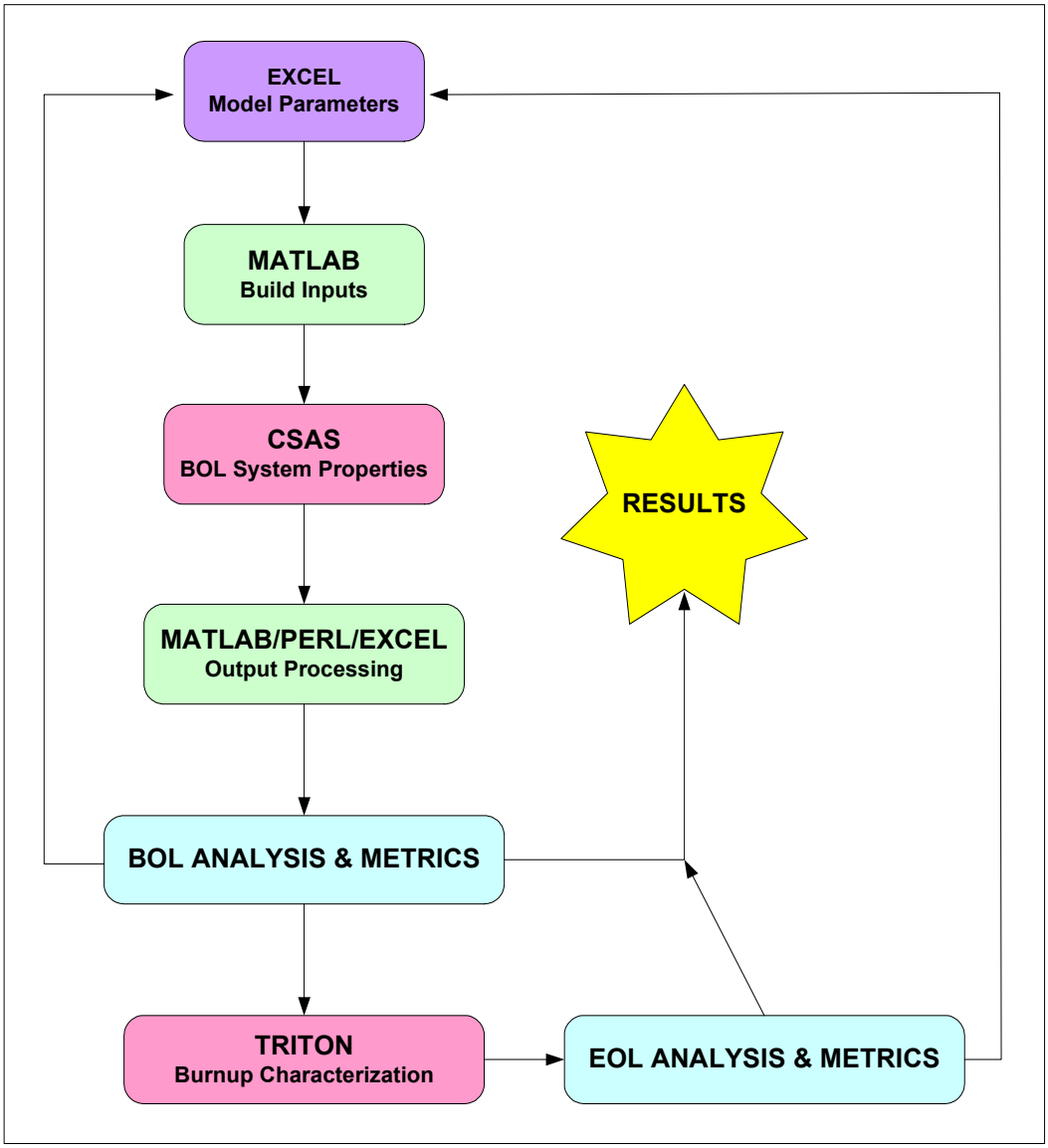

Fig. 4. Applied computer code system.

II.B CSAS25

Criticality Safety Analysis Sequences (CSAS) were developed for the SCALE code system to provide automated, problem-dependent, cross-section processing followed by the calculation of a modeled system neutron multiplication factor. CSAS25 is a one of several control sequences within CSAS that uses KENO V.a to evaluate criticality of 3D systems. CSAS25 is used exclusively in this research for the determination of VHTR performance characteristics at the beginning of life (BOL). CSAS25 allows for near-explicit accounting for lattice effects due to double heterogeneity features that are characteristic for all HTGRs including VHTRs.

Double heterogeneity can be thought of as a double-level geometry. In VHTRs, the first geometry level is formed by randomly–distributed TRISO-coated particles within a graphite matrix of the fuel compact. The second level is formed by a regular hexagonal lattice of fuel compacts within fuel blocks. A special treatment must be used for such systems because of substantial differences in neutron distributions at each heterogeneity level. Each compact has a fuel region containing thousands of micro-particles that form a universe, which clearly exhibits features of an infinite lattice by itself. Only peripheral particles feel the presence of neighboring compacts. As a result, the core neutron distribution is formed by neutron media within each compact and then at the block and the whole core levels.

Fig. 5 illustrates the SCALE double heterogeneity treatment as it is executed in CSAS25. When CSAS25 is executed in SCALE 5.1 for models that contain double heterogeneity cell data (e.g., VHTRs), several functional modules are called upon, including [27]:

1. BONAMI performs unresolved resonance self-shielding calculations for nuclides that have Bondarenko data associated with their cross sections,
2. WORKER creates an AMPX working format library from a master format library,
3. CENTRM uses a pointwise continuous cross-section library (with 10,000 to 70,000 points) and a cell description to generate a pointwise continuous flux spectrum by solving the Boltzmann transport equation for a 1-D spherical or cylindrical system. This module provides necessary capabilities for cross section weighting to account for double heterogeneity lattice effects,
4. PMC using the pointwise continuous flux spectrum created in CENTRM, collapses pointwise continuous cross sections to a set of multigroup cross-sections over primarily the resolved resonance range that can be used by KENO, XSDRNPM, or TRITON,

5. XSDRNPM — provides cell-weighted cross-sections based on the specified unit cell and can calculate the k-eff for a 1-D system by several methods, most importantly in this thesis via the S_n method that is best used for systems that have many regions of dissimilar cross-sections (e.g. compacts). In the SCALE double heterogeneity treatment XSDRNPM is used solely to compute multiplication characteristics for lattices of particles and compacts. It is not used in the actual working library generation process. The CENTRM is used to account for double heterogeneity effects,
6. ICE — creates a single combined homogenized point cross-section library from libraries created by PMC, CENTRM, and BONAMI for use by KENO V.a,
7. CHOPS — computes pointwise flux disadvantage factors and creates homogenized point cross-sections,
8. WAX — creates a combined working library of homogenized cross-sections,
9. CAJUN — combines homogenized point cross-section libraries,
10. AJAX — removes unused mixtures from the final master library, and
11. KENO V.a — calculates k-effective of a 3-D system as well as the modeled system's nuclear characteristics (e.g. fluxes).

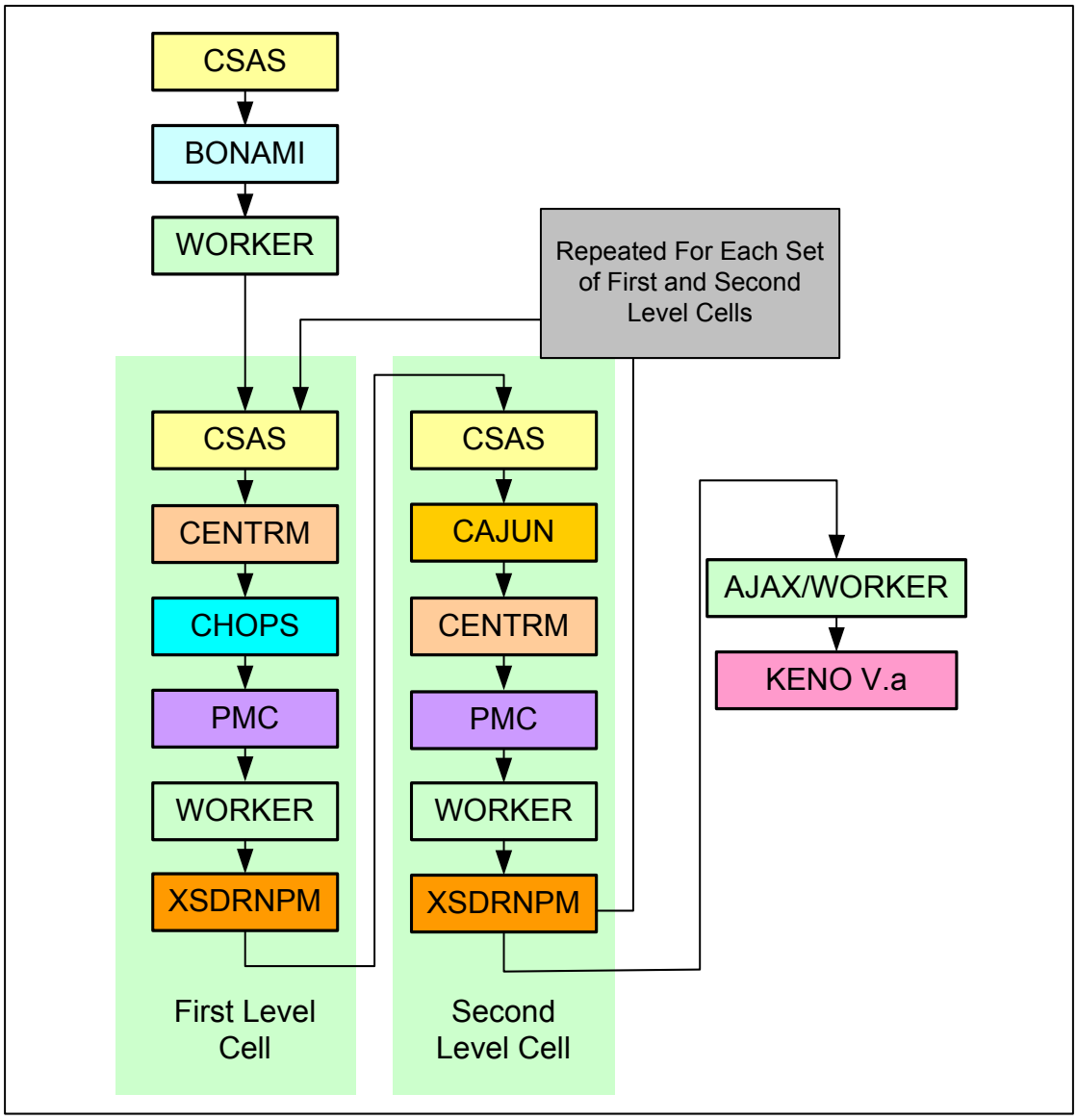

Fig. 5. CSAS25 sequence for double heterogeneous VHTR model.

II.C TRITON

TRITON was developed to handle 2D and 3D depletion scenarios such as axial enrichment of Boiling Water Reactors (BWRs) and the ring effect associated with strong absorbers. There are a total of 5 TRITON sequences, each one having unique abilities while sharing common subroutines. In this research, the TRITON T5-DEPL sequence was used with a modification to allow for depletion of double heterogeneous materials. This sequence uses the KENO V.a functional module at the 3D whole-core modeling level. As illustrated in Fig. 6, the standard SCALE 5.1 TRITON sequence was expanded to add the double heterogeneity processing [27].

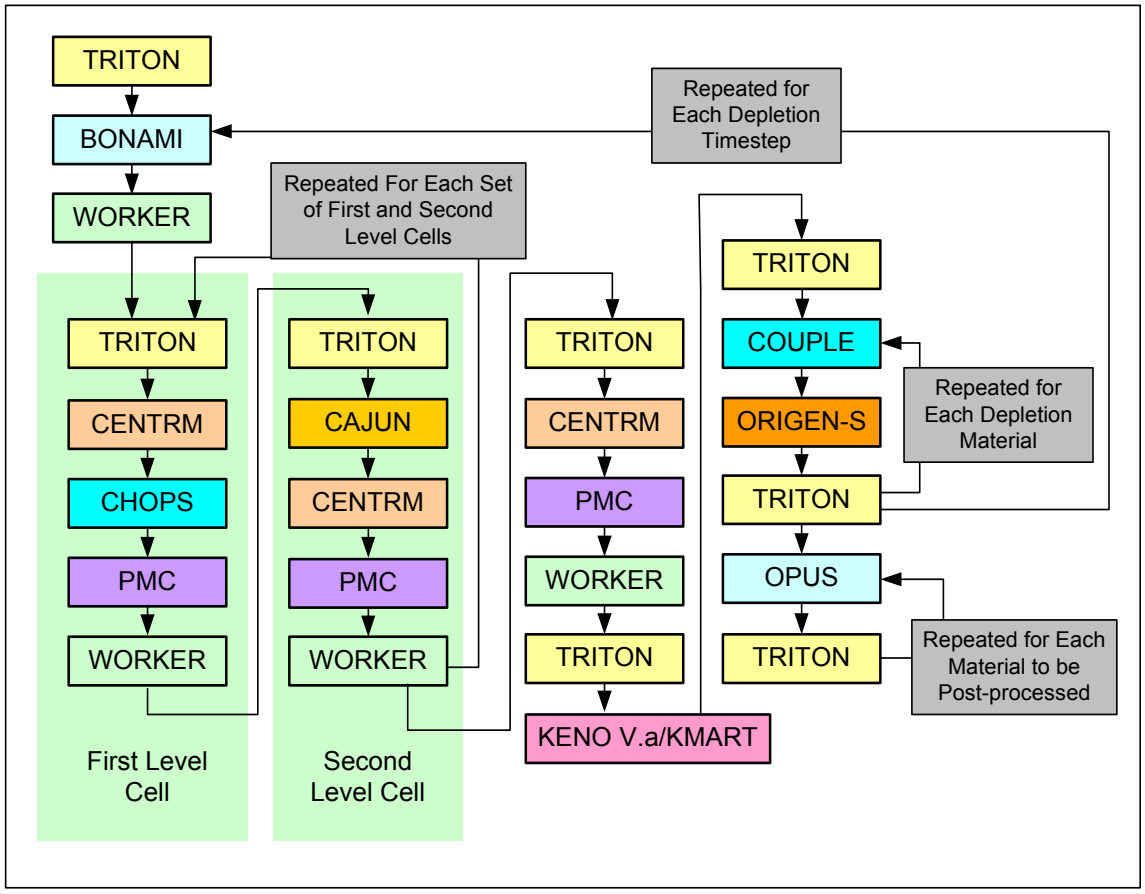

Fig. 6. Modified SCALE TRITON sequence with double heterogeneity processing.

II.D SCALE Limitations

CSAS25 was developed to use simple input data and prepare problem-dependent cross-sections for use in calculating the effective neutron multiplication factor of a 3-D system using KENO V.a. Some of the limitations of the CSAS25 sequence are the result of using preprocessed multigroup cross sections. Other limitations, due to assumptions in the Nordheim integral treatment as implemented in CSAS, can be eliminated by using CENTRM/PMC as the resolved resonance processor. The CENTRM/PMC is used in the present analysis. Limitations in CSAS25 are as follows:

1. Two-dimensional (2-D) effects, such as fuel rods in assemblies where some positions are filled with control rod guide tubes, burnable poison rods and/or fuel rods of different enrichments, cannot be accounted for at the lattice level of the working library processing. The cross sections are processed as if the rods are in an infinite lattice of identical elements. These effects are then accounted for at the whole-core modeling level, and
2. Cannot model annular fuel rods for second level cells, equivalent cylindrical fuel rods must be used, and
3. Maximum number of cross-sections (based on available memory) limits the depth of details allowed for in a model.

The SCALE TRITON T5-DEPL sequence was developed to use simple input data and allow for 3D depletion using KENO V.a and ORIGEN-S. Some of the limitations of the sequence are the result of using ORIGEN-S [27].

III. VHTR PRISMATIC CORE MODEL

The following section describes how a 3D full-core model of a power-size VHTR configuration was created. Though, there are no power-size VHTRs built, there is an abundance of data provided for HTGRs and smaller prototype VTHRs (e.g., HTR10 and HTTR) as well as expected design criteria for power-size VHTRs. The model for this research was developed to take advantage of the robust capabilities of SCALE 5.1, including the complexity of adding a temperature distribution to the model. This temperature distribution for the VHTR model can be obtained by the addition of more materials and regions. This is exemplified in the most complex model, where a total of 511 different materials were used to encompass major features of a VHTR. These features range from graphite blocks to the individual coatings of TRISO particles. The sequential creation of SCALE inputs and their corresponding output required an automated process. This process was managed through a Matlab script, that was capable of producing and managing the creation of inputs and analyses of their corresponding outputs by reading and recording model parameters in excel files [27].

III.A 3D Whole-Core Model of a Power-Size VHTR

The geometry of the VHTR was created for use with SCALE 5.1 sequences focusing on KENO V.a. at the whole-core modeling level. The model created is a near exact depiction of the expected physical description of a power-size VHTR. The fundamental building blocks of the reactor (e.g., fuel blocks and its constituents) and the ratio of these blocks (i.e,. control rod guide blocks to fuel block ratio) to one another are based on HTTR design parameters [28], while the overall configuration of the reactor has been developed following the DOE VHTR design requirements [21, 19, 18, 23]. The final core layout showing the VHTR fuel and reflector locations is shown in Fig. 7.

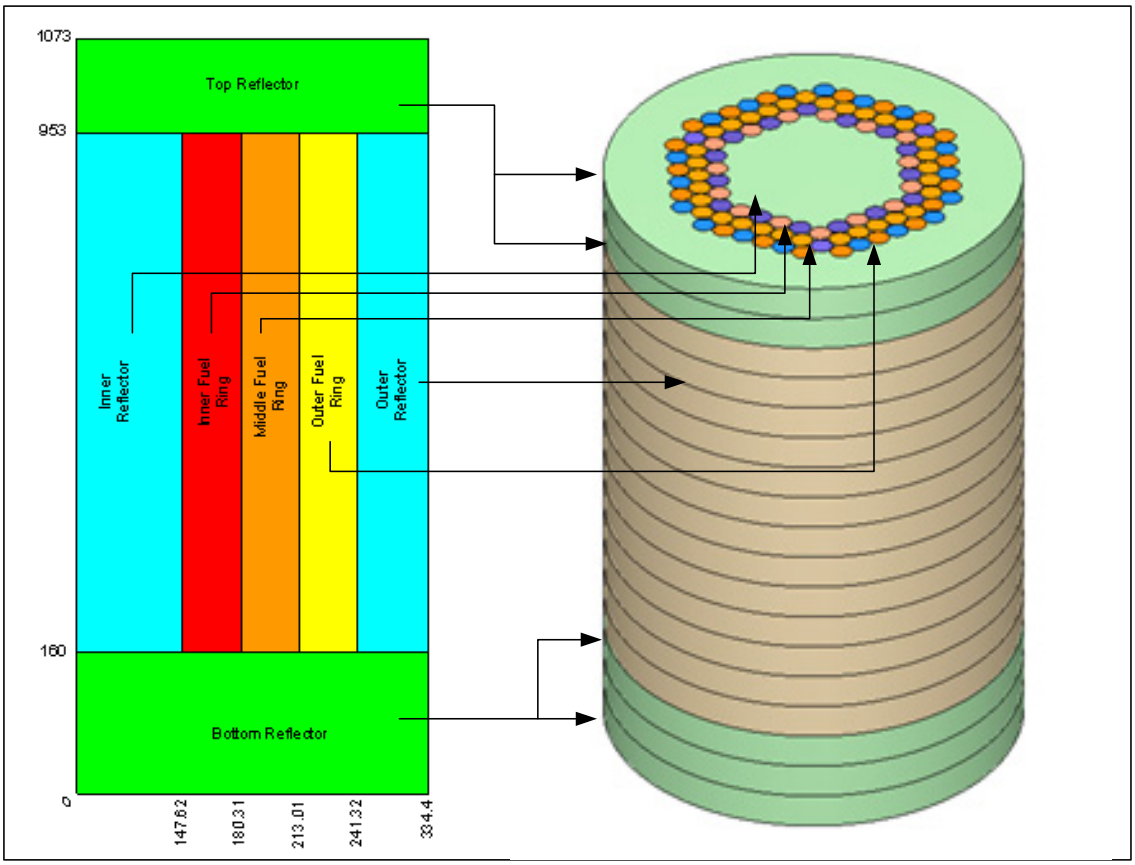

Fig. 7. 3D whole-core model of a power-size VHTR.
figure not to scale, dimensions in cm

KENO V.a allows for a large assortment of elementary shapes, whose combination allow for complex geometries to be modeled. The blocks modeled for this research were adapted to the limitations of KENO V.a. The adaptation made was to model individual blocks as cylinders (shown as green in Fig. 8) and then place these in a larger graphite structure (shown as red in Fig. 8). Though this is not an exact representation of the hexagonal fuel blocks, the same triangular pitch is used for placing all fundamental blocks in the core and, since each fundamental block is created from the same graphite base materials as the graphite that surrounds the graphite cylinders, the amount of graphite in the VHTR model is conserved. Fuel elements within each block, and in the

core, are arranged in a triangular lattice following the VHTR hexagonal geometry exactly by computing fuel element's 3D coordinates.

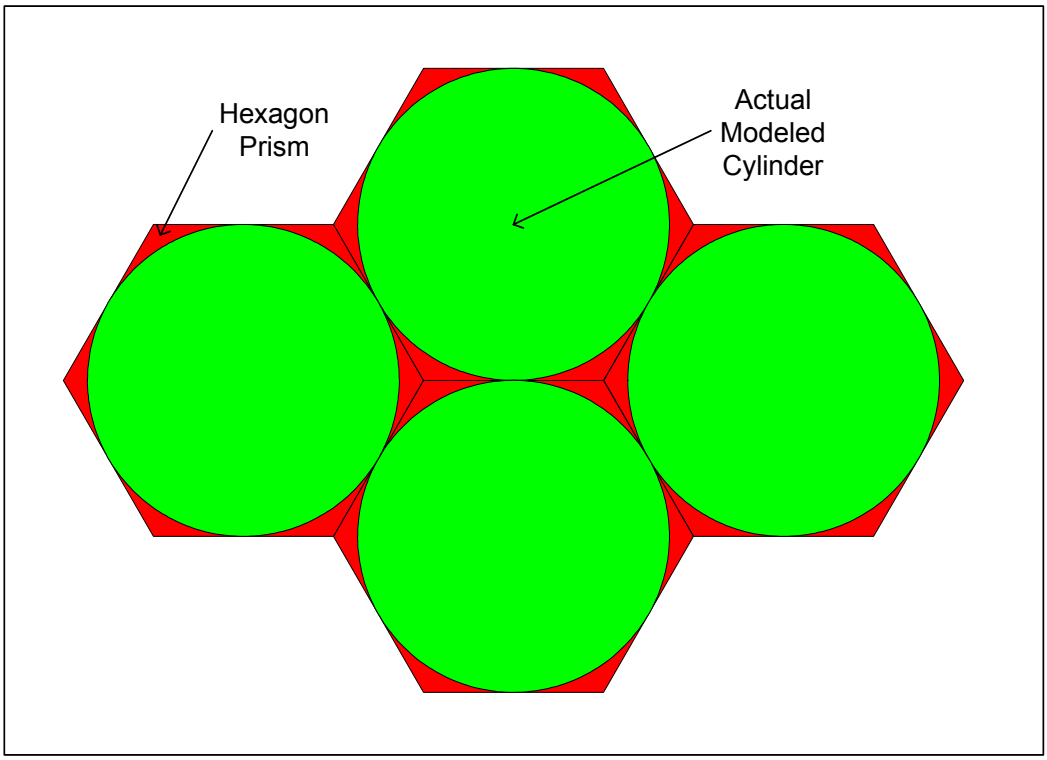

Fig. 8. Hexagon prismatic blocks modeled as cylinders.

The VHTR is built from a combination of three distinctive/fundamental building blocks. These basic blocks (fuel block, coolant block, and control rod guide block) are given a local temperature distribution depending on each block function and location within the model. Each basic block is built from an identical cylindrical graphite block that has had a handling hole bored into the top surface. Basic blocks are differentiated from one another by the addition of bore holes whose size and number are related to the blocks purpose as shown in Fig. 9.

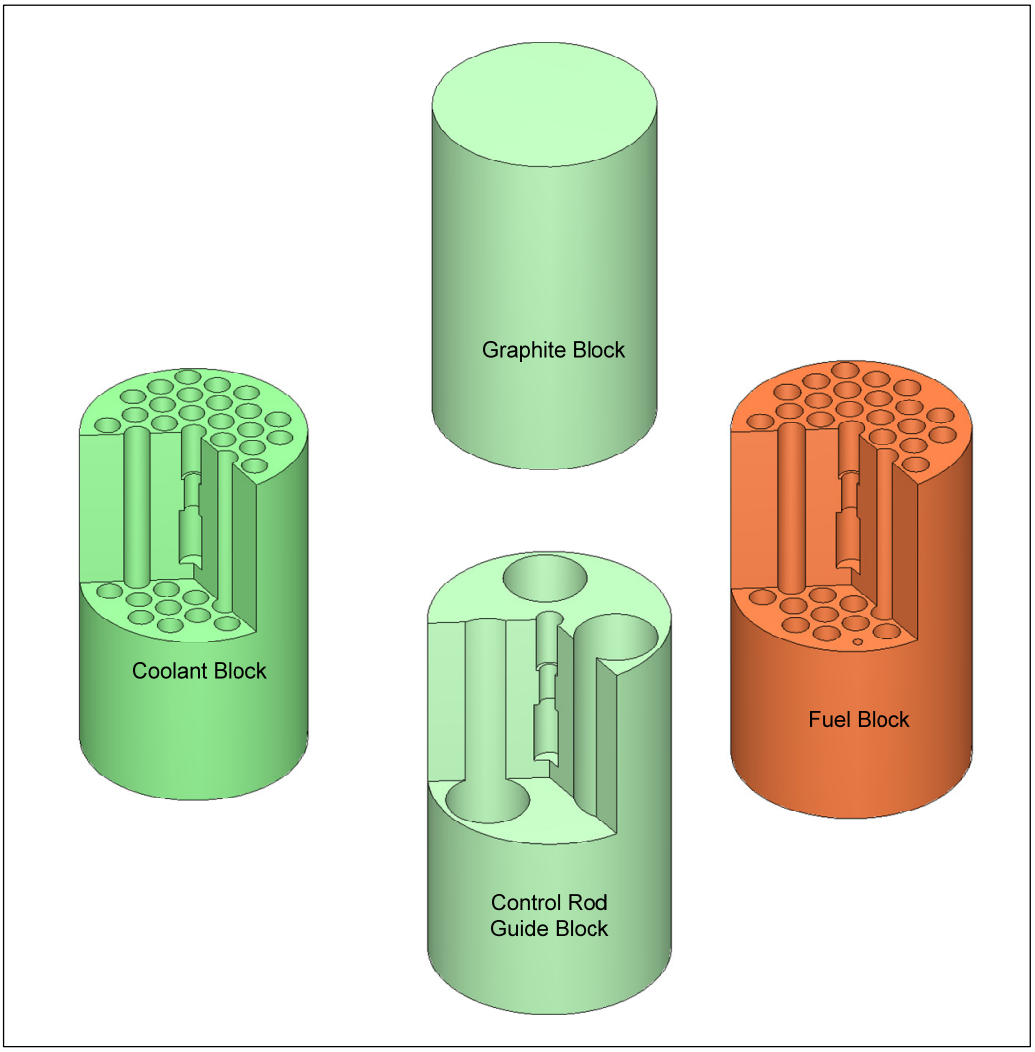

Fig. 9. A graphite block and the three fundamental blocks (as modeled).

III.A.1 Fuel Block

In a prismatic core, all fissile and fertile material is placed in TRISO particles. The particles are placed in a graphite compact, located in a larger hexagonal graphite prism (fuel block). The modeled fuel block is composed of seven essential components: a large graphite cylindrical block, annular fuel rods surrounding helium channels, graphite fuel rod sleeves, coolant channels surrounding the graphite sleeves, a handling hole, and burnable poison rods. Fuel blocks are arranged in three or four rings depending on the

core configuration, shown in Fig. 1. These rings surround a central graphite reflector are stacked upon each other to a height of 13 blocks. All fuel blocks have a radius of 17.9 cm and a height of 58 cm [28]. There are a total of 31 fuel rods placed in the block with room for an additional two fuel rods. The locations of these two optional fuel rods can be placed in regions of the block that are currently modeled as solid graphite. This is shown in Fig. 10. The design details are given in Table IV.

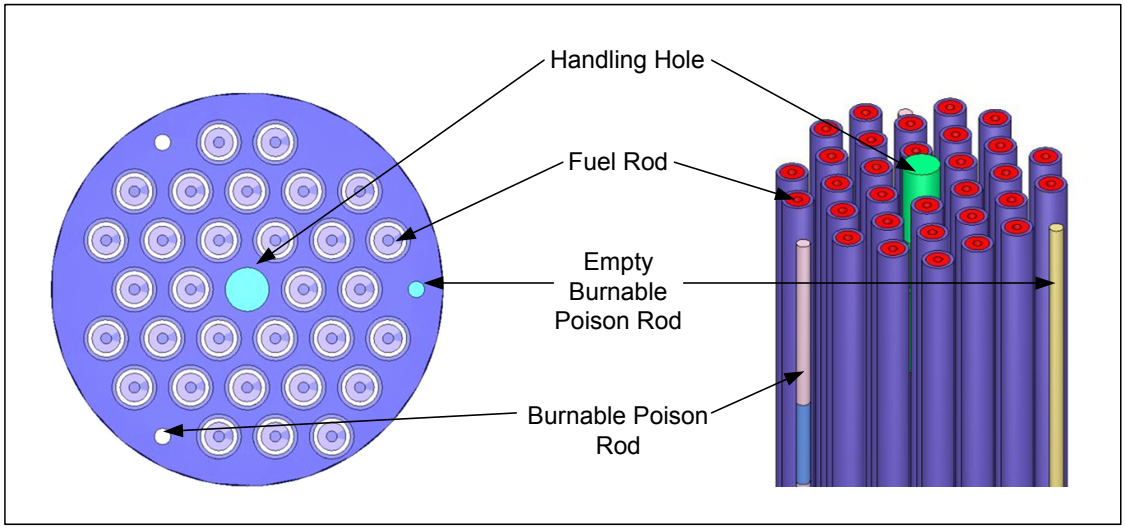

Fig. 10. Fuel block layout.

Table IV. Fuel Block Design Data

Type	Pin-in-Block
Configuration	Cylindrical
Material	Graphite
Density	1.76 g/cc
Impurities	Boron
Height	58
Width Across Flats	36
Number of Fuel Holes in Block	31
Fuel Hole Diameter	4.1 cm
Fuel Hole Height	58.0 cm
Number of Burnable Poison Holes	3
Burnable Poison Hole Diameter	1.5 cm
Burnable Poison Hole Height	50.0 cm

Fuel rods are 54.6 cm tall, have a 0.5 cm radius inner cylindrical void of helium, followed by a series of axial stacked compacts (modeled as a single rod as shown in Fig. 11) that extends to a radius of 1.3 cm. The compact contains TRISO particles encapsulated by a graphite matrix. The compact is enveloped by a graphite sleeve that extends to 1.7 cm, and finally by a layer of coolant to an outer radius of 2.05 cm. This arangement is shown in Fig. 11 and the properties are shown in Table V.

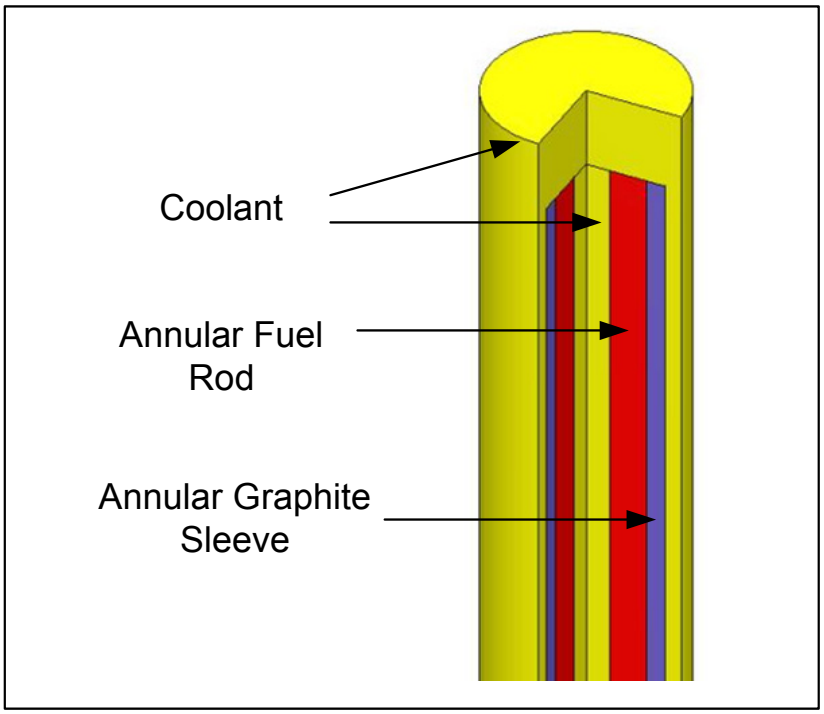

Fig. 11. Fuel rod and coolant channel.

Table V. Fuel Rod/Graphite Sleeve Properties

Fuel Compact	
Number of Fuel Particles	Varies
Graphite Matrix Density	8.54E-2 atoms/barn-cm
Graphite Boron Impurity Density	1.07E-7 atoms/barn-cm
Inner Diameter	1.0 cm
Outer Diameter	2.6 cm
Effective Height of Fuel Rod	54.6 cm
Graphite Sleeve	
Material	Graphite
Graphite Density	1.76 g/cc
Graphite Impurity	Boron
Inner Diameter	2.6 cm
Outer Diameter	3.4 cm
Height	54.6 cm

In the center top of a fuel block there is a handling hole composed of three helium filled cylinders stacked on each other. Proceeding from the top to bottom, the radius of the cylinders start at 2 cm, then 1.5 cm, and finally a 2.25 cm . The top cylinder extends down 9 cm, the next an additional 6 cm, while the bottom helium cavity extends a final 10 cm, giving a full height of the handling hole of 25 cm as shown in Fig. 12. The helium inside the handling though modeled, is not neutronically important but was modeled for completeness.

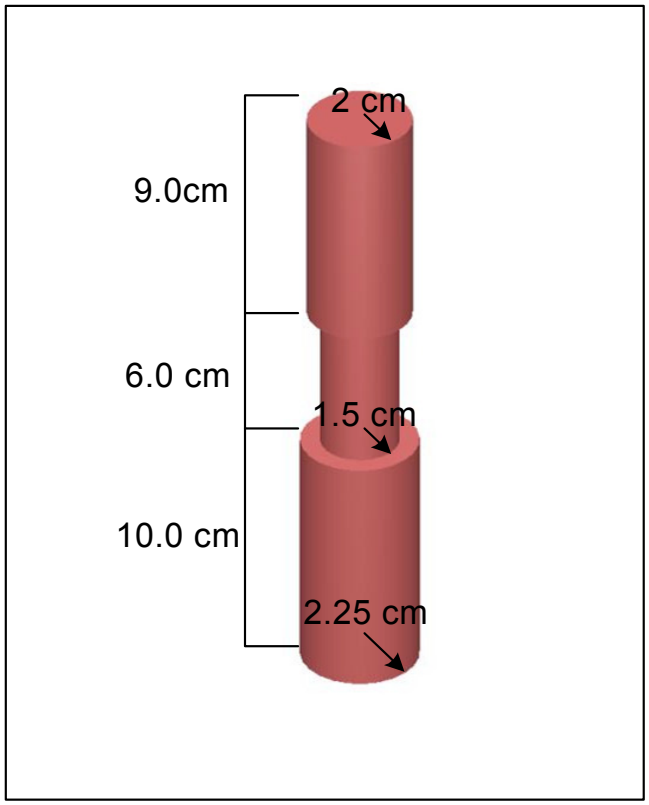

Fig. 12. Handling hole filled with helium.

There are a total of three burnable poison holes in each fuel block, two of which contain burnable poisons while the third is filled with helium. Each cylindrical hole is 50 cm in length starting at 4.2 cm from the bottom of the fuel block, with a radius of 0.75 cm. The holes containing BP contain two individual BP rods, one positioned at the top of the

cavity while the other is placed at the bottom, each extending to a height of 20 cm and axially separated by a graphite plug as shown in Table VI.

Table VI. Burnable Poison Rod Properties

Number of Burnable Poison Holes Available	3
Number of Burnable Poison Holes Used	2
Number of Burnable Poison Holes Unused	1
Burnable Poison Rods in A Hole	2
Height of Burnable Poison Rods	20 cm
Height of Gap Between Burnable Poison Rods	10 cm
Burnable Poison	B_4C
Material Between Burnable Poison Rods	Carbon
Material in Empty Burnable Poison Hole	Helium

Compacts (modeled as annular fuel rods) were filled with TRISO particles at varying volume fractions and varying fissile fuels for this research. Though a multiple of different fuels were analyzed for this research, only one TRISO particle configuration was modeled based on TRISO particles used in the HTTR. Each particle had a dioxide fuel containing boron impurities with an atom density of 7.25×10^{-02} atom/barn-cm, and four coatings slisted in Table VII.

Table VII. TRISO Particle Specifications

Parameter	**Dimensions [cm]**	**Mix Number**
Fuel Radius	0.030405	1
Coating 1 Thickness	0.00587	2
Coating 2 Thickness	0.00292	3
Coating 3 Thickness	0.00287	4
Coating 4 Thickness	0.00456	5
Compact Graphite Matrix	n/a	6
Name	**Mix Number**	**Atom Density [atom/barn-cm]**
Fuel (X-Dioxide)	1	7.25E-02
Graphite	2	5.73E-02
Graphite	3	9.42E-02
Silicon	4	4.81E-02
Carbon	4	4.81E-02
Graphite	5	9.74E-02
Graphite	6	8.54E-02
Boron-10	6	2.12E-08
Boron-11	6	8.55E-08

III.A.2 Control Rod Guide Block

Control rod guide blocks were composed of identical-sized graphite blocks and handling holes as found in the fuel block, but differed by the absence of the fuel and BP holes and the presence of control rod guide holes. There were three control guide holes placed evenly in the block. These guide holes were modeled as cylindrical, helium-filled cavities that extended the full height of the block and had a radius of 6.15 cm, as shown in Fig. 13.

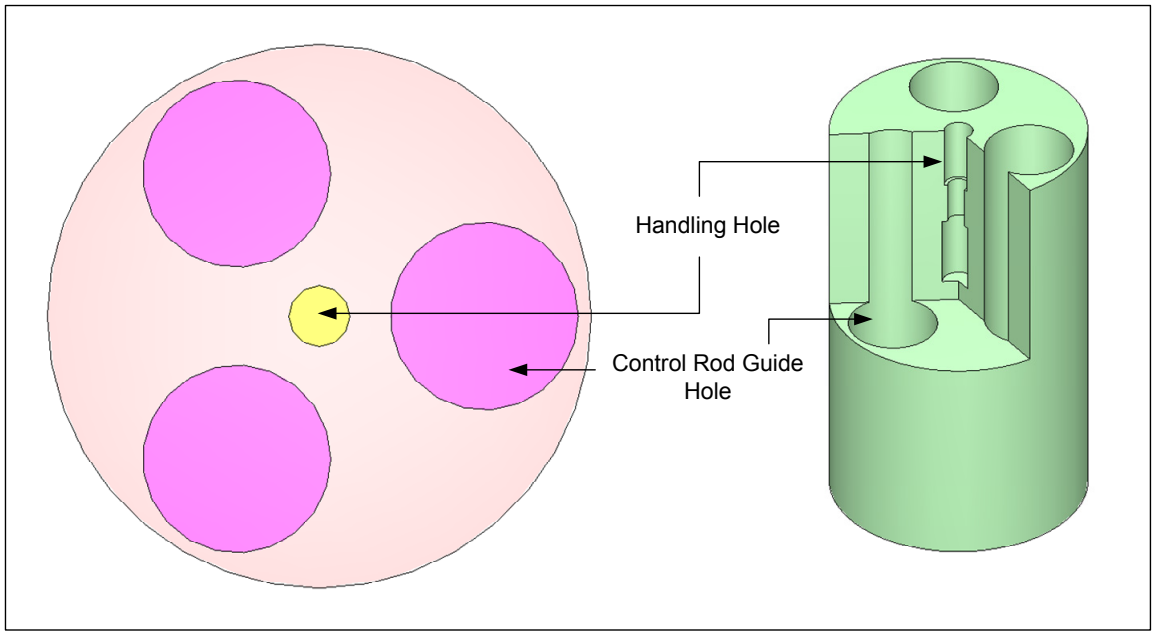

Fig. 13. Control rod guide block.

III.A.3 Coolant Block

Coolant blocks are nearly indistinguishable from fuel blocks, but they lack BP holes and instead of fuel holes they contain coolant holes in the same location that the fuel holes would have been placed. Coolant holes extend the full height of the block and are hollow cylinders filled with helium with a 2.05 cm radius as shown in Fig. 14.

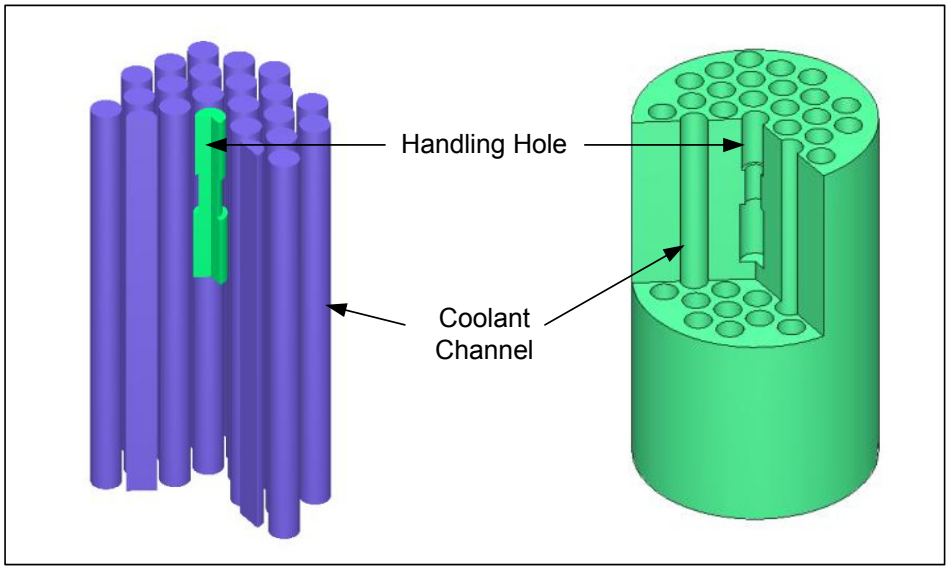

Fig. 14. Coolant block.

III.A.4 Active Core and Reflector

The modeled VHTR system is subdivided into the active core and reflector regions. The active core is annular in shape and composed of a combination of fuel and control rod guide blocks placed in a 3 or 4 ring configuration. The active core is surrounded by inner and outer reflectors that extend from below the active core to above it. The fuel and control rod guide blocks are stacked axially to a height of 754 cm by placing a total of 13 fuel/control block upon each other. In the case of the three ring configuration a total of 66 fuel blocks are placed in a single axial layer. With 13 layers this brings a total of 858 fuel blocks in the active core. In this configuration there are 36 control rod guide blocks placed throughout each axial layer for a total of 468 in the entire active core.

As stated above, the active core surrounds an inner reflector and itself surrounded by an outer reflector. The inner reflector is modeled as a solid graphite cylinder that extends from below the active core to above it. Though the reflector is modeled as a cylinder, it represents solid graphite blocks with the same dimensions as all other fundamental

blocks, as to create a tight triangular pitched array. The only assumption made in modeling the reflectors was not to model the solid graphite blocks with handling holes. In this viewpoint that the reflector is composed of individual solid graphite blocks, the inner reflector stretches 9 blocks across at its maximum width and then reduces to a width to a minimum of 5 blocks. This best demonstrated in Fig. 15.

Table VIII. Reference VHTR Parameters vs. as Modeled

Parameter	Referenced Values	(3/4 Ring Configuration)
Active Core Shape	Annular	Annular
No. of Fuel Columns	102	102/126
Active Core Height	7.93 m	7.93 m
Core Effective Inner Diameter	2.96m	2.96/2.33 m
Core Effective Outer Diameter	4.83 m	4.83 m
Top Reflector Height	1.2 m	1.2 m
Bottom Reflector Height	1.6m	1.6 m
Outer Reflector Diameter	6.88 m	6.8 m

The outer reflector surrounds the active core and extends the same length as the inner reflector, as well as extends above and below the active core. The outer reflector above and below the active core is composed of control rod guide blocks and coolant blocks. There are a total of 330 coolant blocks and 180 control rod guide blocks Outside the active cores radius the outer reflector is modeled as an annular cylinder that extends from the active core out to a radius of 3.4 meters. The space surrounding the outer reflector is modeled as a void. Comparison of the referenced VHTR and the modeled VHTR parameters are shown in Table VIII.

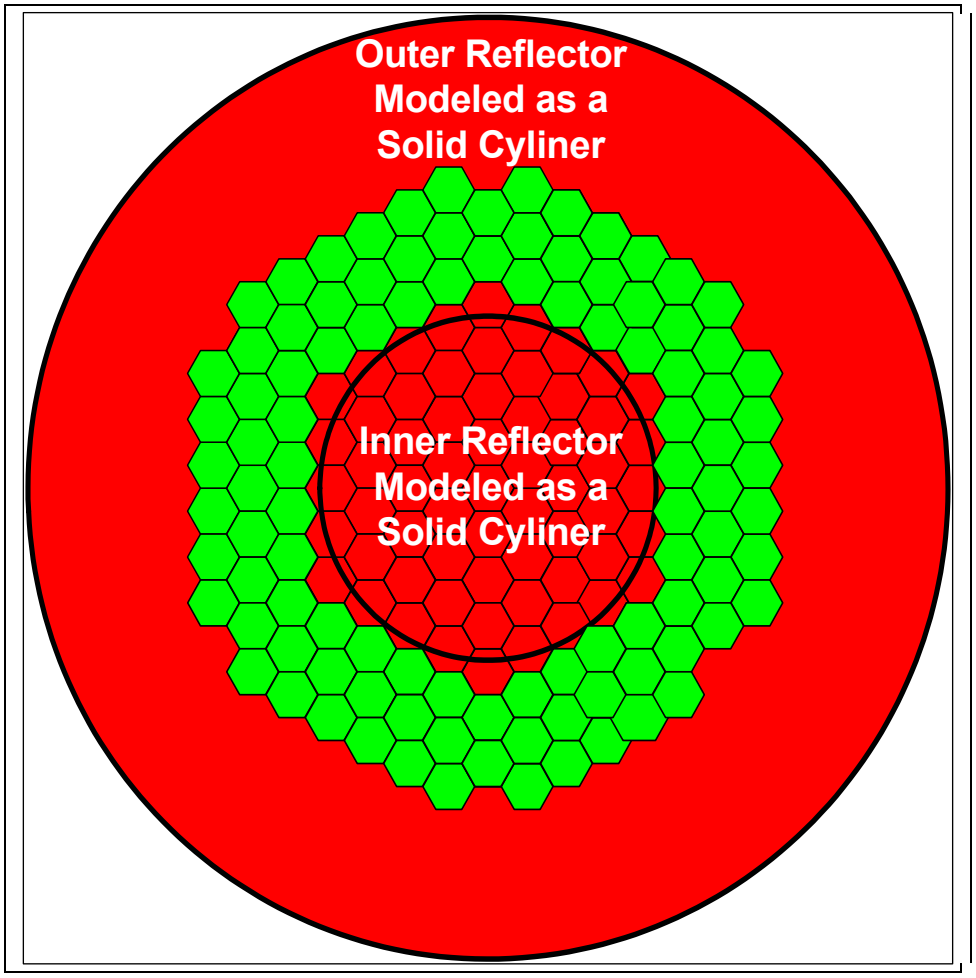

Fig. 15. Reflector representation in the VHTR model.

III.B Temperature and Coolant Flow Model

The temperature distribution for the CSAS VHTR model is based on work done for the thermal response of VHTR [15]. The general model characteristics are summarized in the Table IX:

Table IX. VHTR Temperature Derivation Information

PARAMETER	VALUE	UNITS
Core Thermal Power	600	MW
Helium Flow Rate through the Core	320	kg/s
Avg. Helium inlet/outlet temperature	490/1000	C
Core inner and outer avg. Diameter	2.96/4.84	m
Core Height	8	m
Average Active Core Temp.	~1300	K

This information was evaluated and a general temperature distribution was created within the limits of CSAS25 (e.g. memory limit). Fig. 16 gives the temperature distribution developed for the three fuel-ring VHTR configurations used in CSAS25 models. For the four fuel-ring configuration, the inner two rings were given the same temperature distribution as that given to the inner ring in the three fuel-ring configuration.

The inner and outer reflectors have three radial regions and fifteen axial regions. The top reflector has three axial regions and nine radial regions while the bottom has two axial regions and the same nine radial regions. The active core is composed of a total of thirteen axial and three radial regions. To reduce the model due to memory allocation limits associated with the SCALE 5.1, more than one region was modeled with the same material. This is the case with graphite blocks within the active core. With thirteen axial and three radial regions, a total of 39 temperature varying graphite blocks would be needed to fully capture the available detail allowed for in the model. Due to the limitations, the axial temperature distribution in the core is reduced to nine regions but the three radial regions were retained. Thus, in the active core, only 27 temperature unique graphite blocks were used.

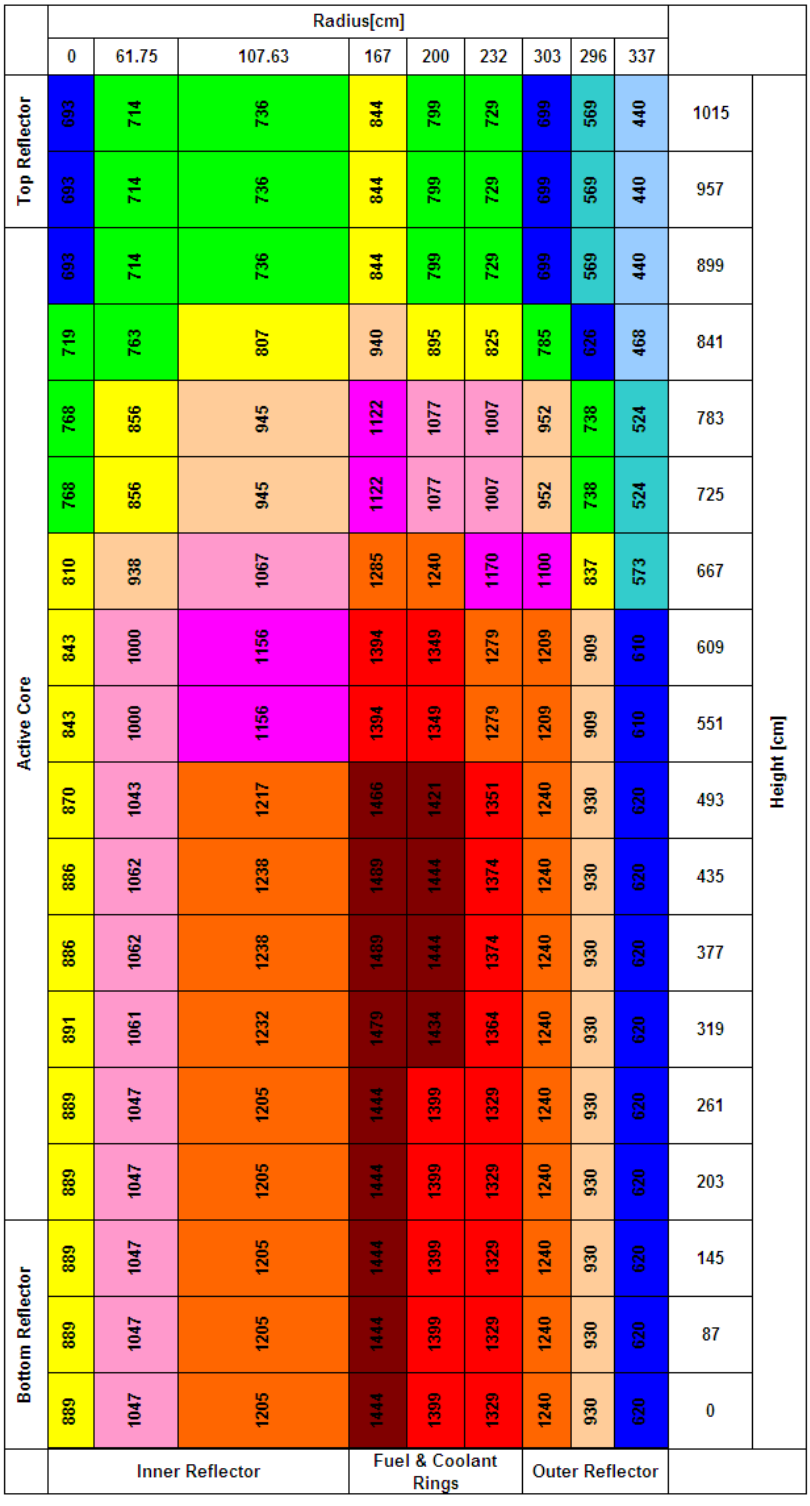

Fig. 16. 3D temperature distribution in the VHTR model.

The coolant flow is shown in Fig. 17. It was assumed that more graphite would be needed in regions of higher temperatures to dissipate residual decay heat in a loss of coolant accident.

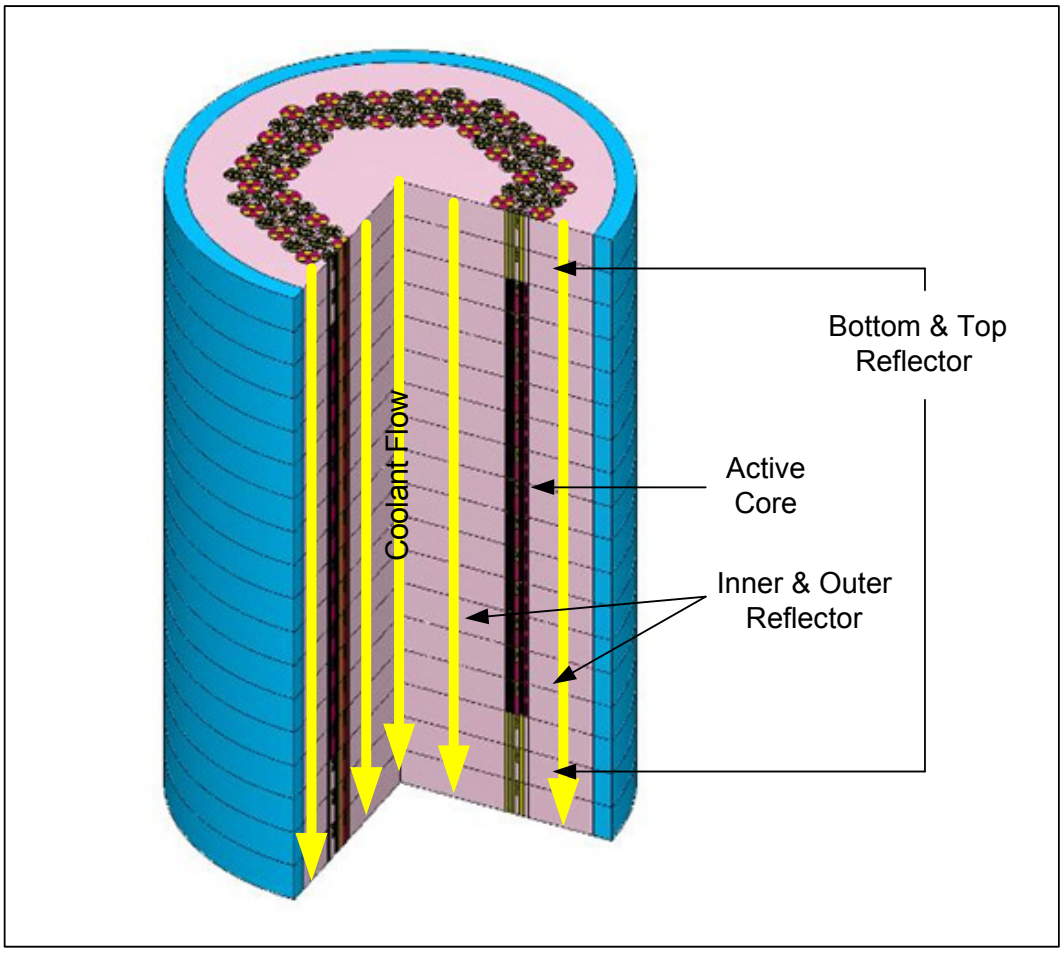

Fig. 17. Coolant flow in the VHTR model.

III.C Transmutation Efficiency Analysis Model

One of the objectives of this research was to analyze the transmutation capability of LWR SNF compositions in extended-life VHTRs. To facilitate this analysis, a fuel-cycle scheme had to be created. The potential of recycling and reprocessing of spent fuel involves partitioning and separating nuclides into various waste streams that can either be reused as fuel or placed in a geological repository. With the wide variety of UREX systems currently being investigated, it has been assumed that a UREX or a UREX-derivative system will be available when VHTRs come online that will have the capability of near perfect efficiency in the separation of U, TRU, and FPs from LWR waste streams. Fig. 18 shows the envisioned fuel cycle and the LWR waste streams expected. In this figure, a PWR element with a fuel loading of 3.75% enriched uranium is burnt for 41,200 MWd/MTHM and cooled for 23 years is reprocessed into TRU and LEU fuel forms. Table X gives the expected waste streams that are produced from a UREX stream and are used this research as the basis of fuel compositions.

There are basically two neutron reactions of interest in transmutation. The first is neutron capture, which when occurring with actinides generally leads to more actinides and fission. Fission for some actinides (e.g., Am-244) is much more likely with fast neutrons and, more generally, fission is more likely with fast neutrons. This is where applicability of VHTRs is demonstrated. As discussed in the introduction, the use of TRISO-coated micro-particles allows for flexible fuel loadings and for variable C/HM ratios. Fig. 19 shows how a TRU-fueled VHTR can have its neutron spectrum changed by changing the C/HM ratio.

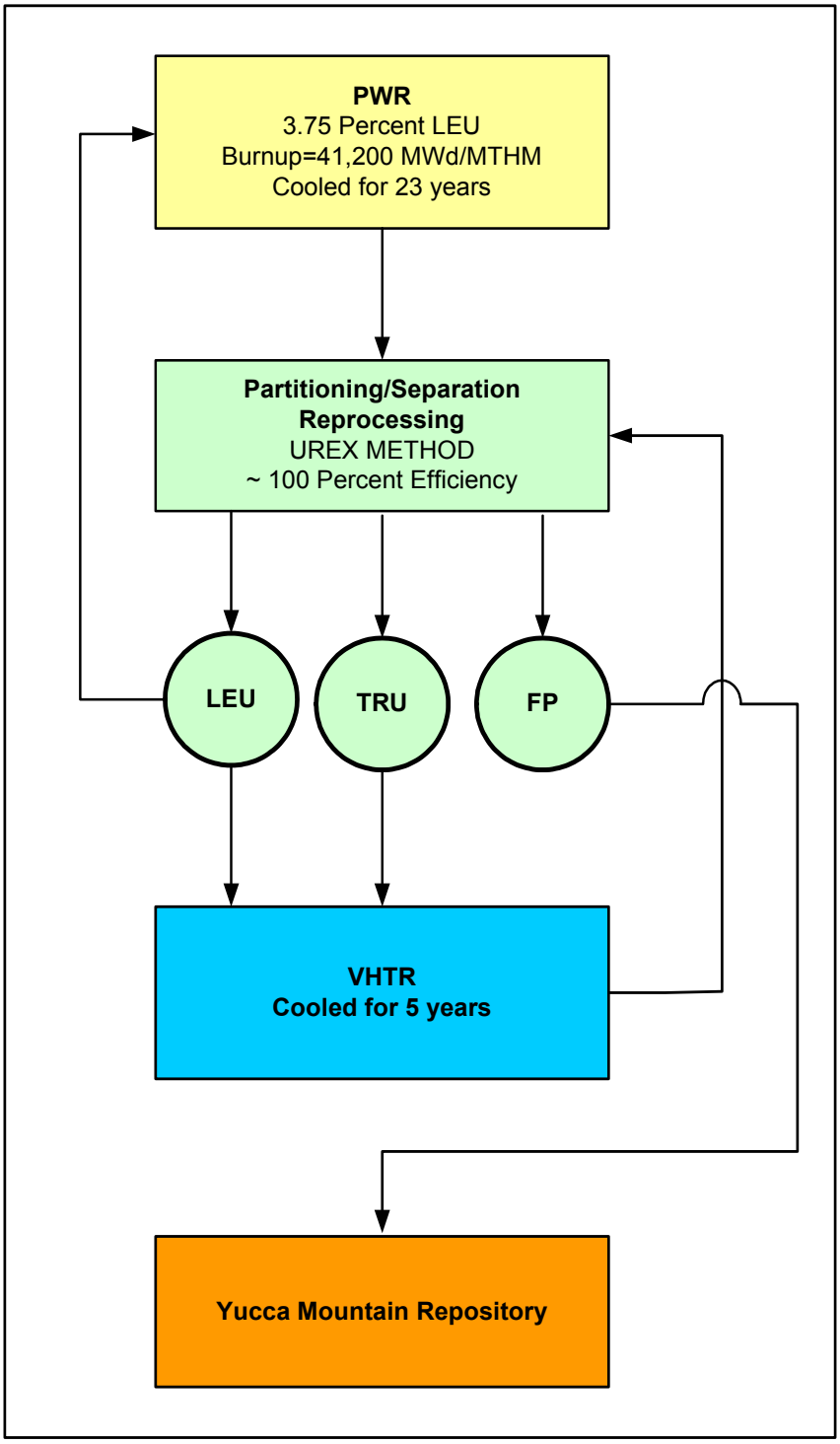

Fig. 18. VHTR fuel cycle.

Table X. Expected Waste Streams from PWR Fuel Reprocessing

Reactor Grade Plutonium (RGPu) Vector		
Element	**Nuclide**	**Composition (atom %)**
Plutonium	Pu-238	2.36
	Pu-239	61.453
	Pu-240	26.022
	Pu-241	4.877
	Pu-242	5.289
Total		100
Transuranic (TRU) Vector		
Element	**Nuclide**	**Composition (atom %)**
Neptunium	Np-237	6.121
Plutonium	Pu-238	1.986
	Pu-239	51.718
	Pu-240	21.899
	Pu-241	4.104
	Pu-242	4.451
Americium	Am-241	8.25
	Am-242m	0.02
	Am-243	1.23
Curium	Cm-243	0.003
	Cm-244	0.194
	Cm-245	0.021
	Cm-246	0.003
Total		100
Minor Actinide (MA) Vector		
Element	**Nuclide**	**Composition (atom %)**
Neptunium	Np-237	38.635
Americium	Am-241	52.079
	Am-242m	0.127
	Am-243	7.762
Curium	Cm-243	0.021
	Cm-244	1.225
	Cm-245	0.134
	Cm-246	0.017
Total		100

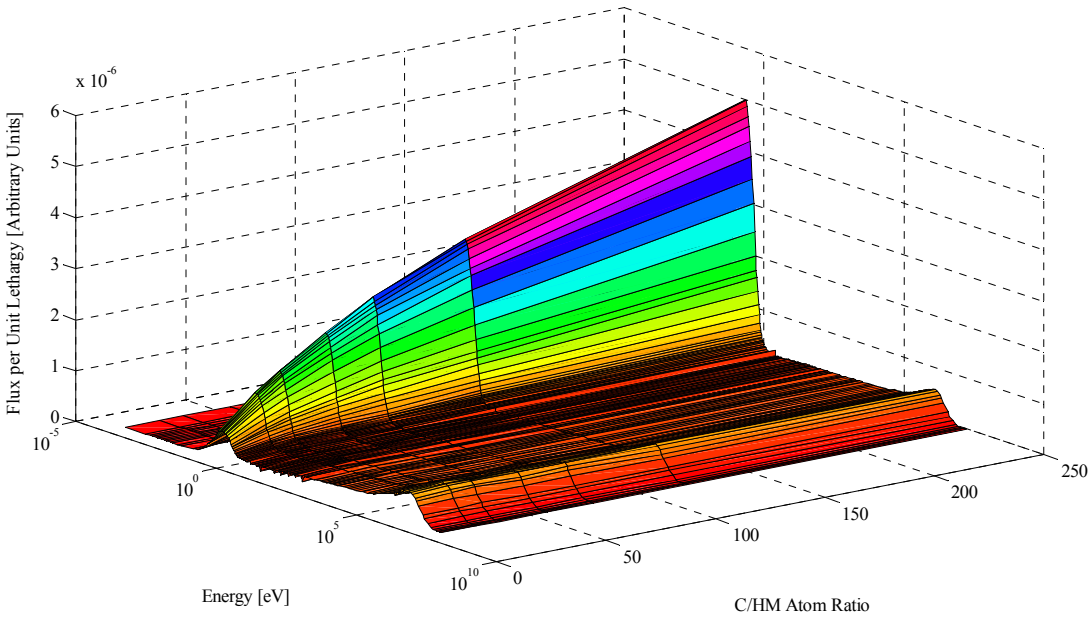

Fig. 19. Specturm shifting via C/HM variations.

The C/HM ratio was calculated per compact, knowing the TRISO geometry, fuel rod geometry, and the compact material makeup in Table XI.

Table XI. TRISO Particle Composition

Material	Region	Atom Density [atom/b-cm]
Heavy Metal	Fuel	2.41E-02
C (Graphite)	Coating-1	5.73E-02
C (Graphite)	Coating -2	9.42E-02
Si (Free Gas)	Coating -3	4.81E-02
C (Free Gas)	Coating -3	4.81E-02
C (Graphite)	Coating -4	9.74E-02
C (Graphite)	Compact-Matrix	8.54E-02
B-10	Compact-Matrix	2.12E-08
B-11	Compact-Matrix	8.55E-08

Knowing this information, it is possible to determine the amount of carbon and heavy metal is present in a TRISO particle. Knowing that TRISO particles compose a specific volume fraction (VF) of each compact, then a carbon to heavy metal ratio can be calculated for a given compact since the volume of a single TRISO-particle (V_{TRISO}) is known. By knowing the atom densities of carbon in each coating of a TRISO particle, the carbon atom density in the matrix, as well as the HM atom density in a the TRISO particle, the following equations can be used to obtain a C/HM ratio.

$$\frac{VF \cdot \mathrm{C}_{TRISO} + \left(1 - VF\right) \cdot \mathrm{C}_{MATRIX}}{\mathrm{VF} \cdot HM_{TRISO}}$$

$$C_{TRISO} = \sum_{n=1}^{4} \frac{V_{coating-n}}{V_{TRISO}} \rho_{coating-n}^{C-atom} = 4.22\text{E-}02$$

$$HM_{TRISO} = \frac{V_{fuel}}{V_{TRISO}} \rho_{fuel}^{HM-atom} = 6.68E-03$$

With this knowledge, C/HM can be calculated by knowing the VF of TRISO particles in a compact shown in Table XII.

Table XII. VF to C/HM Atom Ratio

Volume Fraction	C/HM Atom Ratio
0.1	121.32
0.2	57.43
0.3	36.13
0.4	25.48
0.5	19.09
0.6	14.84
0.7	11.79

Transmutation efficiency was computed in this research as a percent of TRU destruction (Percent Net TRU-Destruction) as well as judged on the exiting waste stream radiotoxicity. The first metric is important since the Congress mandated capacity was limited to 70,000 MTHM that can be placed in the Yucca Mountain. The second metric limit is based on the maximum heat-load (11.8 kW/canister) a HLW canister can have when emplaced into the Yucca Mountain. The relationship is:

$$\text{Net TRU-Destruction \%} = \frac{MTHM_{BOL} - MTHM_{EOL}}{MTHM_{BOL}} \quad .$$

III.D In-Core Fuel Cycle Analysis

In-core fuel cycle studies for this research include characteristics describing the VHTR performance during its operation:

1. Parameters of the initial fuel loading including
   a. Transuranic content
   b. Uranium content
   c. Plutonium content
   d. Minor actinide content
2. Carbon–to-heavy metal atom ratios for compacts
3. k_{eff} at BOL
4. Fuel cycle length
5. Energy spectra and fast fluences
   a. Core average
   b. Fuel rod average
   c. TRISO (coatings and kernel)
6. Net fissile-fuel production and consumption
7. Net fertile-fuel production and consumption

Initial fuel loading is a BOL parameter necessary before any calculations are done. Since these loadings are known, the amount of fissile and fertile nuclides can be determined in each VTHR as well as the radiotoxity of the fuel at BOL. Carbon to heavy metal atom ratios for compacts will be compared for each fuel and used to judge its effect on core life and TRU burnup. K_{eff} at BOL is calculated using CSAS25 and is used for the evaluation of what core configurations have acceptable BOL k_{eff} for depletion in TRITON. Fuel-cycle length is the most important metric to the objective of this research and is measured as the point at which the k_{eff} of the core falls below 1.0. Energy spectra are evaluated due to their importance for core reactivity stabilization during operation, TRISO failure rate evaluations, as well as TRU transmutation efficiency calculations. The final two metrics, net fissile-fuel production and

consumption and net fertile-fuel production and consumption are important measurements as to whether the waste stream leaving the VHTR will be usable as fuel after reprocessing.

IV. PERFORMANCE ANALYSIS OF TRU-FUELED VHTR SYSTEMS OPERATING IN A SINGLE BATCH MODE

In this section, studies of the VHTR operation domains have been performed using the SCALE 5.1 code package. The system is assumed to be at operational temperature. Both BOL and reactor operation conditions are taken into consideration. The validity of modeling double heterogeneous prismatic graphite reactors with SCALE was determined in previous studies [7]. Specifically SCALE 5 was benchmarked against experimental results obtained in the HTTR program.

IV.A Parametric Analysis at BOL Conditions

In this section, BOL VHTR configurations were analyzed using CSAS25 of the SCALE 5.1 code system. Analysis of BOL cores is important to determine systems with acceptable safety characteristics, as well as a desirable BOL reactivity margins. Further analysis was done to determine system's performance characteristics during operation. All the modeled cores in this section take advantage of both a temperature distribution developed in section III.B.I, as well as the complex modeling techniques allowed for studies using the SCALE code system (see discussion of SCALE limitations in Section II.A.4).

IV.A.1 CSAS25 Double Heterogeneity Treatment

After initial cross section processing, the CSAS25 execution begins with CENTRM calculations of the flux for the first level infinite lattice. For a prismatic VHTR, the first level infinite lattice represents the randomly distributed TRISO particles inside of a graphite matrix. The combination of particles and matrix create the compact. This first level lattice is modeled by CENTRM as an infinite array of TRISO particles in the graphite matrix. Cell-averaged fluxes and flux disadvantage factors are calculated and from these physic parameters, flux-weighted cross-sections are produced. The cross-sections produced for the first level lattice are used in the calculation of the reactor

physics parameters for the second-level lattice. The second-level lattice is modeled using CENTRM as an infinite array of fuel rods, graphite sleeves and coolant channels surrounding the graphite sleeves. Core-wide physic parameters, such as fluxes and multiplication factors, of the system are obtained using KENO V.a.

For comparison, the fluxes calculated during CSAS25 execution at each state of the double heterogeneity treatment are shown in Fig. 20. The CENTRM flux shown for the first level of heterogeneity has a hard spectrum due to the moderation by the TRISO coatings and the interstitial graphite between particles. This is an accurate representation of the energy-dependent flux that would be encountered in a fuel kernel that is not near the edge of a compact (i.e., away from the graphite sleeve). At the second level of heterogeneity, carbon within the compact and graphite sleeves surrounding the compacts are taken into account. The effect is apparent by the well-defined thermal peak. In the calculations at the whole core level, the flux of the compact is calculated using KENO V.a. accounting for the whole core geometry. The accounting of the graphite at the whole core modeling level has a significant effect on the magnitude of the thermal peak, which now is the dominant feature of the energy-dependent flux. The change in magnitude of this peak from when CENTRM was used to calculated the compact's spectrum to the spectrum calculated using KENO V.a, demonstrates that significant moderation is occurring outside the compact and graphite sleeve. The final neutron spectrum, as shown in Fig. 20, was calculated for the graphite fuel block.

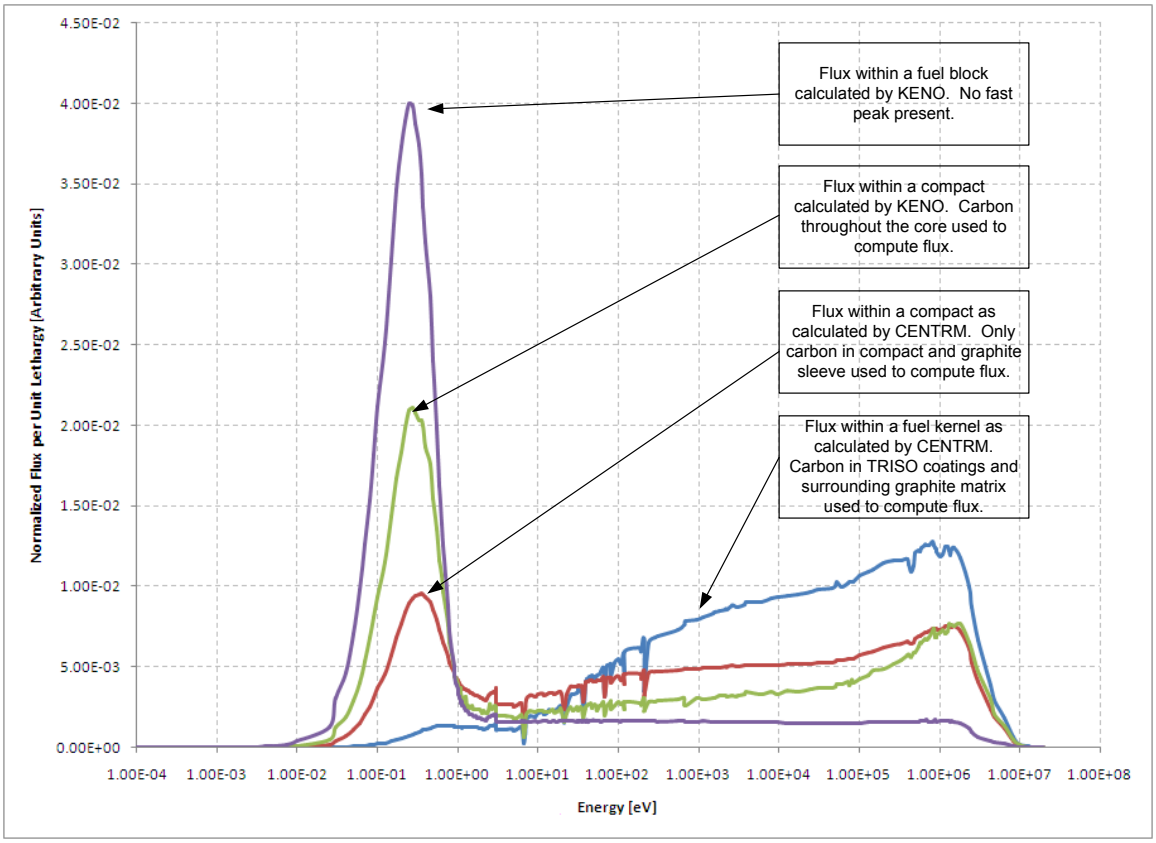

Note: Three fuel-ring LEU VHTR with a C/HM atom ratio of 36 at a height of 464 cm in the inner most fuel-ring.

Fig 20. Fluxes in the VHTR systems at different levels of the double heterogeneity treatment.

An important part of modeling with KENO V.a to analyze VTHRs is its ability to be used to calculate a 3D space-energy neutron distribution. Fig. 21 demonstrates this by showing the flux for a LEU-fueled VHTR as a function of energy and core height for compacts in the innermost fuel-ring. The effects of leakage at the core ends noted by both the decrease in the thermal and fast flux peak magnitude demonstrate that system leakage has a major effect on system behavior, specifically k_{eff}. Comparison of the 3D flux distribution, for a three fuel-ring and four fuel-ring system, shows no principal differences in the flux shape and distribution.

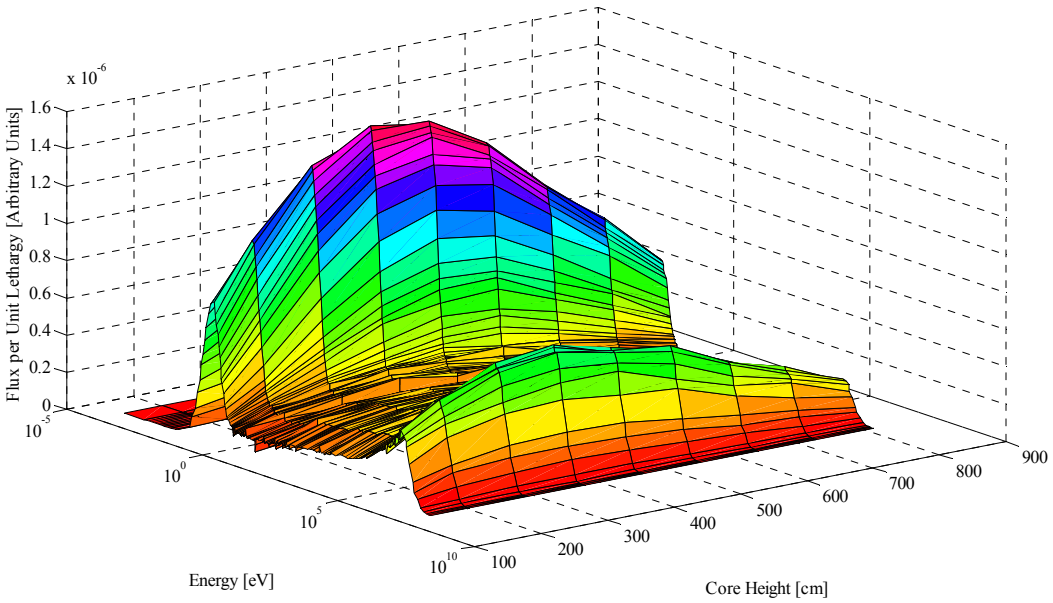

Note: Three fuel-ring LEU (7.92 at %) fueled VHTR with a C/HM atom ratio of 36 in the innermost fuel ring.

Fig 21. 3D space-energy neutron distribution in the VHTR system (neutron fluxes in compacts as a function of their locations in the VHTR core).

IV.A.2 Effects of Fissile Content on LEU-Fueled VHTRs

Quantifying the effect of varying enrichment is important in showing how the ratio of fertile to fissile atoms affects both the neutron multiplication of the system as well as other reactor physics parameters. These effects were quantified for both the three fuel-ring and four fuel-ring core configurations, by analysis of energy of the average neutron lethargy causing fission (EALF), system mean free path, system average neutron fission yield, and effective multiplication factor.

The effect of enrichment on the energy-dependent neutron flux inside the compacts for a LEU-fueled VHTR core is shown in Fig. 22. This figure demonstrates that as a VHTR system moves from a LEU to a HEU fueled configuration, the flux within the compact

gains a harder spectrum, though at a considerably slower rate after an enrichment of 15% is reached.

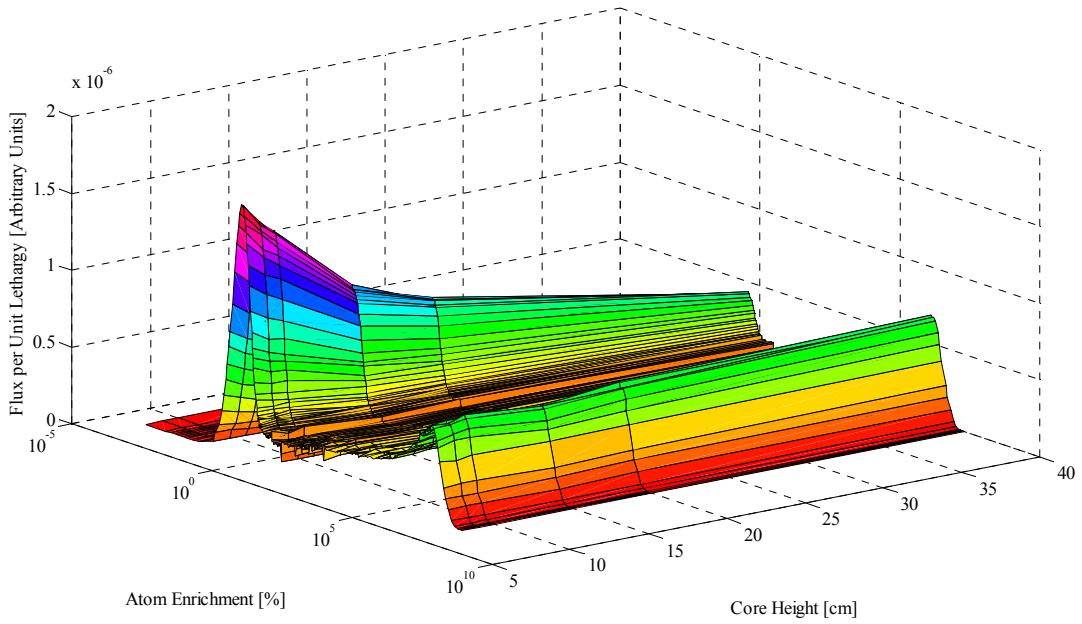

Note: Three fuel-ring VHTR with a C/HM atom ratio of 36 in the inner most fuel-ring at a height of 464 cm.

Fig 22. KENO V.a flux inside a compact as a function of LEU enrichment.

The effect of enrichment on effective multiplication factor (k_{eff}), as well as its effect on other reactor physics parameters, is summarized in Table XII. The relationships between enrichment and k_{eff} for both the three and four fuel-ring core configuration are shown in Fig. 23. After enrichment has increased to approximately 15%, increasing U-235 atom concentration does not drastically change k_{eff}.

The addition of an extra fuel-ring results in a small but constant increase in k_{eff}. This can be attributed to the fact that neutrons born in any fuel block have a much higher chance of causing fission in that same fuel block since the MFP is on the order of centimeters vs. tens of centimeters needed to leave a fuel block. The addition of k_{eff} can be attributed to neutrons leaking inward toward the inner reflector and thus causing fission inside the

additional fuel-ring. A summary of reactor physic parameters for varying LEU enrichments is given in Table XIII.

Table XIII. Reactor Physics Parameters for Three and Four Ring LEU-VHTR Configurations as a Function of LEU Enrichment

Number of Rings	Enrichment	k_{eff}	EALF [eV]	Avg. Neutron Fission Yield	MFP [cm]
3	3	0.863	n/a	n/a	n/a
3	7.92	1.181	0.2188	2.438	1.909
3	9	1.214	0.2316	2.438	1.914
3	10	1.239	0.2463	2.438	1.917
3	15	1.328	0.3168	2.438	1.925
3	20	1.379	0.3994	2.438	1.932
3	40	1.481	0.8380	2.439	1.945
4	3	0.903	n/a	n/a	n/a
4	7.92	1.218	0.2229	2.438	1.830
4	9	1.252	0.2376	2.438	1.833
4	10	1.278	0.2524	2.438	1.835
4	15	1.365	0.3295	2.438	1.845
4	20	1.414	0.4158	2.438	1.853
4	40	1.510	0.8926	2.439	1.869

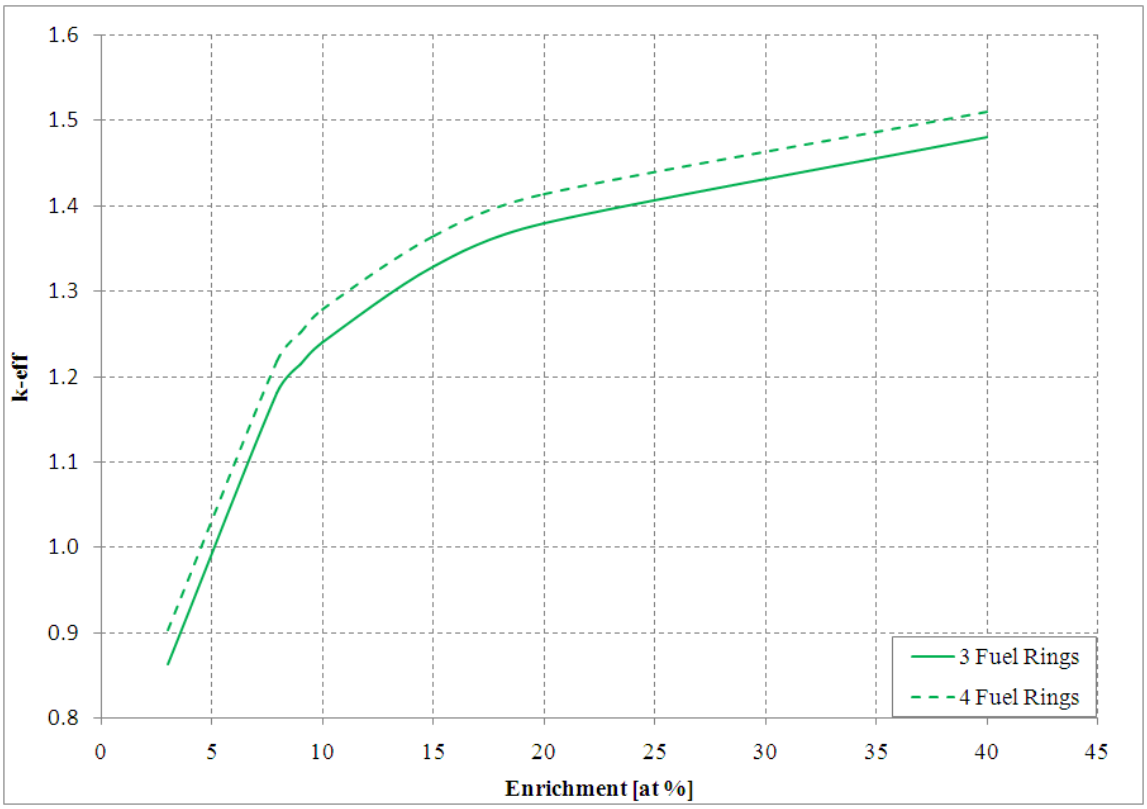

Note: Three and four fuel-ring LEU-fueled VHTR with a C/HM atom ratio of 36.

Fig 23. Keff for three and four fuel-ring LEU-fueled VHTR for varying enrichments

IV.A.3 Effects of Carbon-to-Heavy Metal Ratio on LEU-Fueled VHTRs

The next series of BOL VHTR calculations are used to determine the effects of changing the C/HM atom ratio in LEU systems. This was accomplished by choosing single fuel enrichment and changing the number of TRISO particles in a compact. Fuel enrichment was chosen assuming that it has to yield k_{eff} of approximately 1.2. For the three fuel-ring LEU cases an enrichment of 9% was chosen and 8.7% was chosen for the four fuel-ring cases. The series of CSAS25 calculations is summarized in Table XIV.

Table XIV. Reactor Physics Parameters for Three and Four Ring LEU-VHTR Configurations as a Function of C/HM Atom Ratio

Number of Rings	Enrichment	C/HM	k_{eff}	EALF [eV]	Avg. Neutron Fission Yield	MFP [cm]
3	9	249.10	0.74	n/a	n/a	n/a
3	9	121.32	0.98	n/a	n/a	n/a
3	9	78.73	1.09	0.17	2.44	1.89
3	9	57.43	1.15	0.19	2.44	1.90
3	9	36.13	1.21	0.23	2.44	1.91
3	9	25.48	1.24	0.29	2.44	1.92
3	9	9.51	1.26	0.57	2.44	1.94
4	8.7	249.10	0.78	n/a	n/a	n/a
4	8.7	121.32	1.02	0.15	2.44	1.80
4	8.7	78.73	1.13	0.17	2.44	1.81
4	8.7	57.43	1.19	0.19	2.44	1.82
4	8.7	36.13	1.24	0.23	2.44	1.83
4	8.7	25.48	1.27	0.29	2.44	1.84
4	8.7	9.51	1.28	0.57	2.44	1.86

For three fuel-ring and four fuel-ring systems, as the C/HM atom ratio is reduced, k_{eff} (shown in Fig. 24), EALF, and MFP increase. The reason for this effect is due to the C/HM atom ratio on the energy-dependent flux inside a compact, as demonstrated in Fig. 25. The hardening of the spectrum by the decrease in the C/HM atom ratio is the result of fast neutrons encountering fewer carbon atoms and more HM atoms while traveling through the compact. These neutrons are forced to thermalize outside the compact before causing fission or interacting with HM atoms. The effect of these processes leads to a higher probability of fast-neutron-induced fissions.

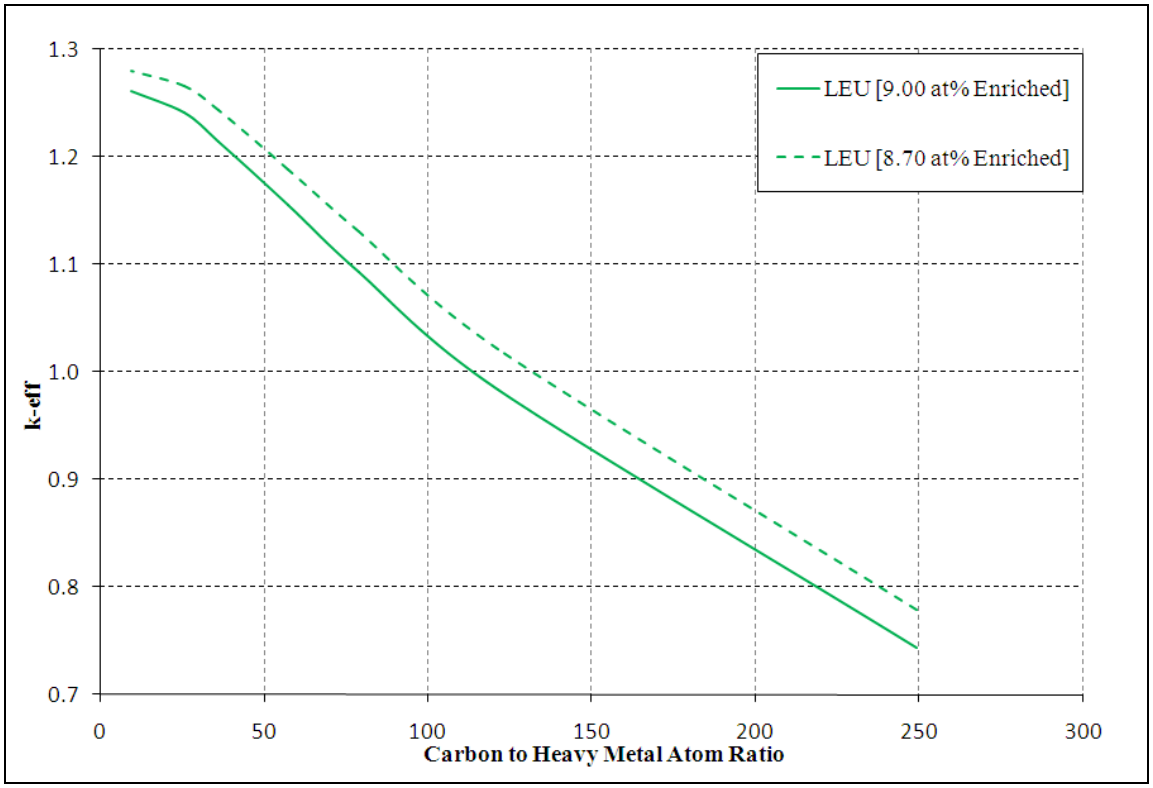

Note: three and four fuel-ring VHTRs fueled by LEU.

Fig 24. K_{eff} for three and four fuel-ring VHTR fueled with LEU for varying C/HM atom ratios

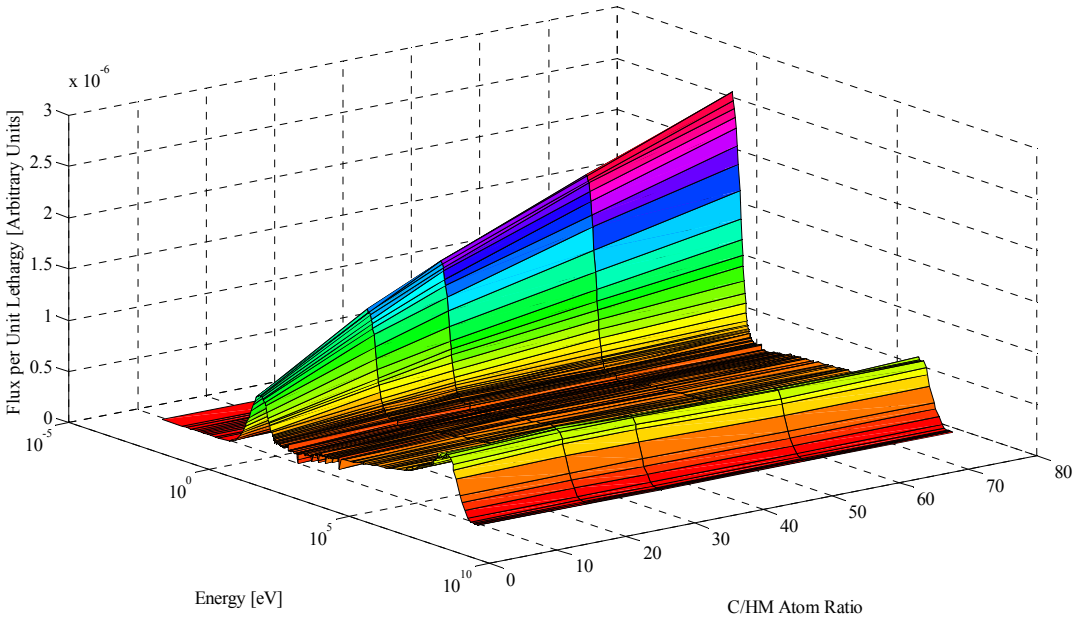

Note: Three fuel-ring VHTRs fueled with LEU. Flux taken from compacts located in the inner most rings at a height of 464 cm.

Fig 25. Energy dependent flux for a three fuel-ring VHTR fueled with LEU for varying C/HM atom ratios

IV.A.4 Analysis of the RGPu-Fueled VHTRs

The operational domains of RGPu-fueled cores were analyzed and compared to TRU-fueled cores. The reason for this comparison is the complex effect of MAs on the energy-dependent cross-sections and flux in TRU compositions. Since fuel compositions with RGPu do not contain MAs, the analysis allows the assessment of effects caused by Pu in TRUs.

Similar to Section IV.A.1, the RGPu cases were analyzed first by keeping the C/HM atom ratio the same (i.e., number of TRISO particles per fuel compact) while changing the amount of fissile content in the fuel kernels. For RGPu, this was done by increasing the amount of RGPu and decreasing the amount of U-238. The reason for this is the assumption that in the fuel cycle envisioned for VHTRs in this research, LWRs would

produce a waste stream with a specific RGPu vector that could not be changed due to proliferation risks and the difficulty in isolating specific Pu isotopes. The results of fissile content variations for both the three fuel-ring and four fuel-ring RGPu-fueled cores are given in Table XV.

Table XV. Reactor Physics Parameters for Three and Four Ring RGPu-VHTR Configurations as a Function of Fissile Content

Number of Rings	Fissile Atom Fraction	k_{eff}	EALF [eV]	Avg. Neutron Fission Yield	MFP [cm]
3	3.32	0.99	n/a	n/a	n/a
3	6.63	1.02	0.37	2.89	1.95
3	9.95	1.04	0.46	2.89	1.96
3	13.27	1.05	0.57	2.89	1.96
3	16.58	1.06	0.69	2.89	1.96
3	19.90	1.07	0.83	2.89	1.96
3	23.22	1.08	0.99	2.89	1.97
3	39.80	1.14	2.05	2.90	1.97
3	59.70	1.22	4.01	2.90	1.97
4	3.32	1.00	0.30	2.89	1.86
4	6.63	1.04	0.38	2.89	1.88
4	9.95	1.05	0.48	2.89	1.88
4	13.27	1.06	0.60	2.89	1.89
4	16.58	1.07	0.74	2.89	1.89
4	19.90	1.08	0.90	2.89	1.89
4	23.22	1.09	1.07	2.89	1.90
4	39.80	1.15	2.30	2.90	1.90
4	59.70	1.23	4.53	2.90	1.90

Similar to the LEU cases, when the amount of fissile content in RGPu-fueled VHTRs is increased, k_{eff}, MFP, and EALF of the system increase as well. The increase in k_{eff} from fissile nuclide increase is much slower in these cases compared to the LEU systems due

the parasitic absorption of fertile Pu being much stronger when compared to U-238. The effect that fissile content has on k_{eff} is illustrated in Fig. 26.

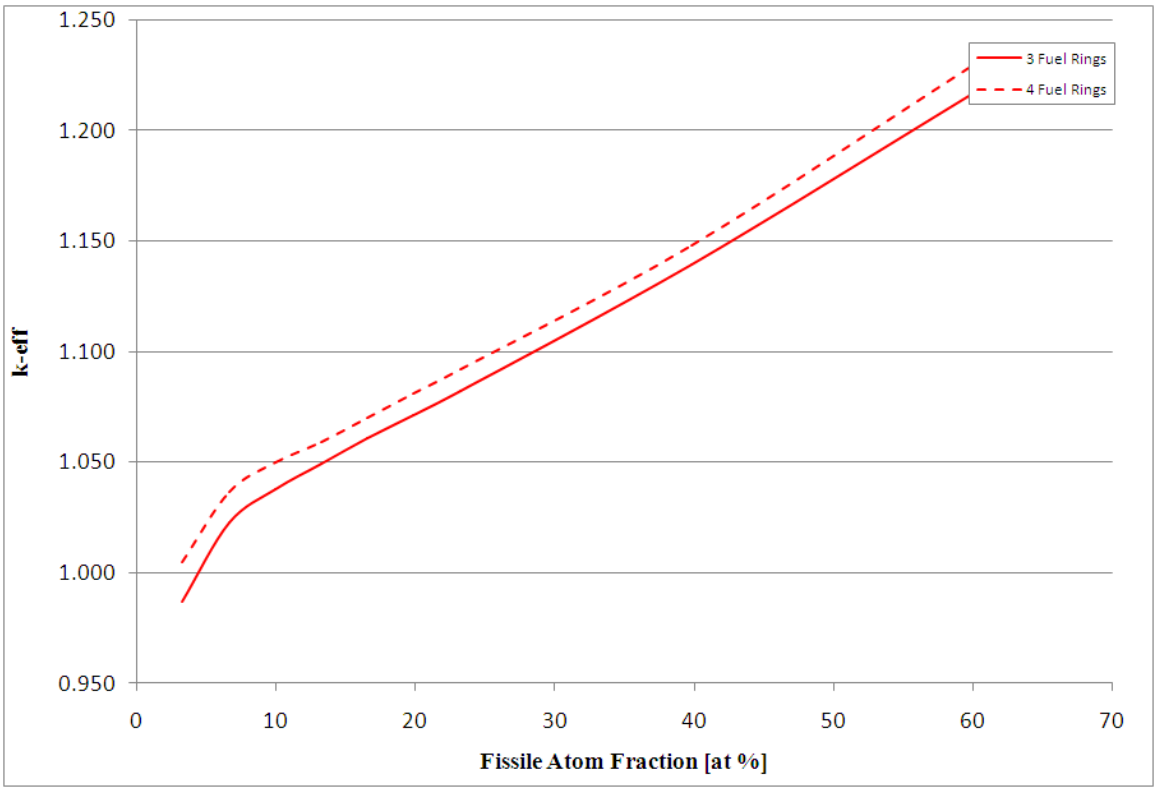

Note: Three and four fuel-ring VHTRs fueled with RGPu with a C/HM atom ratio of 36.

Fig 26. Keff for three and four fuel-ring VHTR for varying fissile atom fractions.

IV.A.5 Analysis of TRU-Fueled VHTRs

The effects of C/HM variations on RGPu-VHTR configurations are analyzed by picking a single fissile atom fraction and changing the number of TRISO particles in a compact. A fissile atom fraction was chosen assuming k_{eff} of approximately 1.2. For the three and four fuel-ring RGPu cases, a fissile atom fraction of 53.06% was chosen. This simplified the comparison of RGPu three ring and four ring cases. For the TRU-fueled cases, k_{eff} of 1.2 wasn't possible at the C/HM atom ratio of 36 (used for the LEU configurations in 4.1.1). As a result, 100% TRU-filled kernels were considered. The

corresponding fissile atom fraction was 55.86%. Table XVI summarizes the results for the RGPu-fueled VHTRs as a function of C/HM atom ratio.

Table XVI. Reactor Physics Parameters for Three and Four Ring RGPu-VHTR Configurations as a Function of C/HM Atom Ratio

Number of Rings	Fissile Atom Fraction	C/HM	k_{eff}	EALF [eV]	Avg. Neutron Fission Yield	MFP [cm]
3	53.064	1271.34	1.07	0.21	2.89	1.90
3	53.064	632.44	1.17	0.24	2.89	1.92
3	53.064	419.47	1.19	0.28	2.89	1.93
3	53.064	312.99	1.19	0.32	2.89	1.94
3	53.064	249.10	1.19	0.36	2.89	1.94
3	53.064	78.73	1.16	1.07	2.89	1.96
3	53.064	50.33	1.17	1.97	2.90	1.97
3	53.064	36.13	1.19	3.29	2.90	1.97
3	53.064	25.48	1.21	5.69	2.90	1.97
3	53.064	19.09	1.24	9.14	2.90	1.97
3	53.064	11.79	1.29	19.50	2.91	1.98
4	53.064	1271.34	1.12	0.21	2.89	1.82
4	53.064	419.47	1.23	0.28	2.89	1.85
4	53.064	249.10	1.21	0.37	2.89	1.86
4	53.064	78.73	1.17	1.16	2.89	1.89
4	53.064	50.33	1.18	2.18	2.90	1.90
4	53.064	25.48	1.23	6.49	2.90	1.90
4	53.064	11.79	1.30	22.83	2.91	1.91

Table XVI shows that as the C/HM atom ratio decreases, the EALF, and the MFP increases. Unlike the LEU cases, however, k_{eff} does not always increase as the C/HM atom ratio decreases. This is illustrated in Fig. 27.

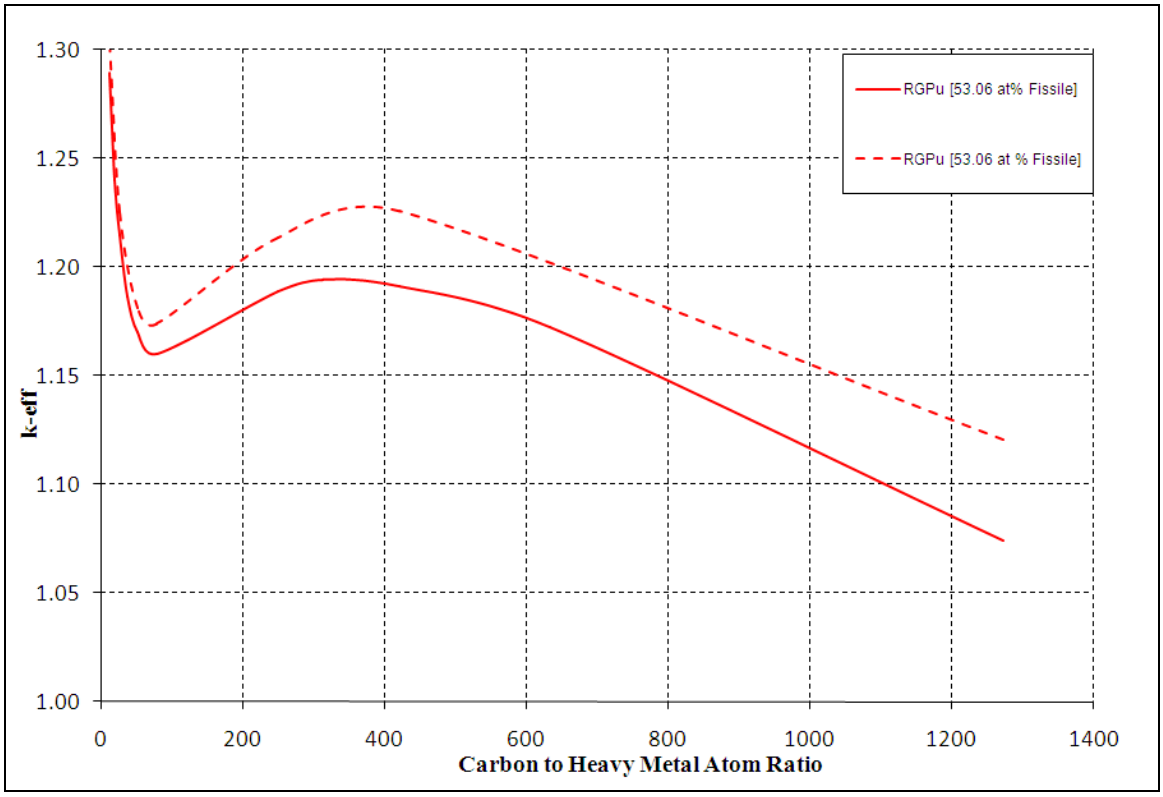

Note: Three and four fuel-ring VHTRs fueled by RGPu.

Fig 27. Keff for three and four fuel-ring VHTR fueled with RGPu for varying C/HM atom ratios.

Fig. 27 shows for a C/HM atom ratio between 75 and 400, there is a transition on how k_{eff} is related to the C/HM atom ratio inside the compact. Table XVI shows that in this range the EALF is far more strongly dependent on the C/HM ration when compared to the for C/HM atom ratio above 400. This is illustrated in Fig. 28. This figure shows that between 400 and 75 C/HM the EALF begins to increase much faster than for a C/HM above 400. When the C/HM falls below 75, EALF begins to increase at an even faster rate.

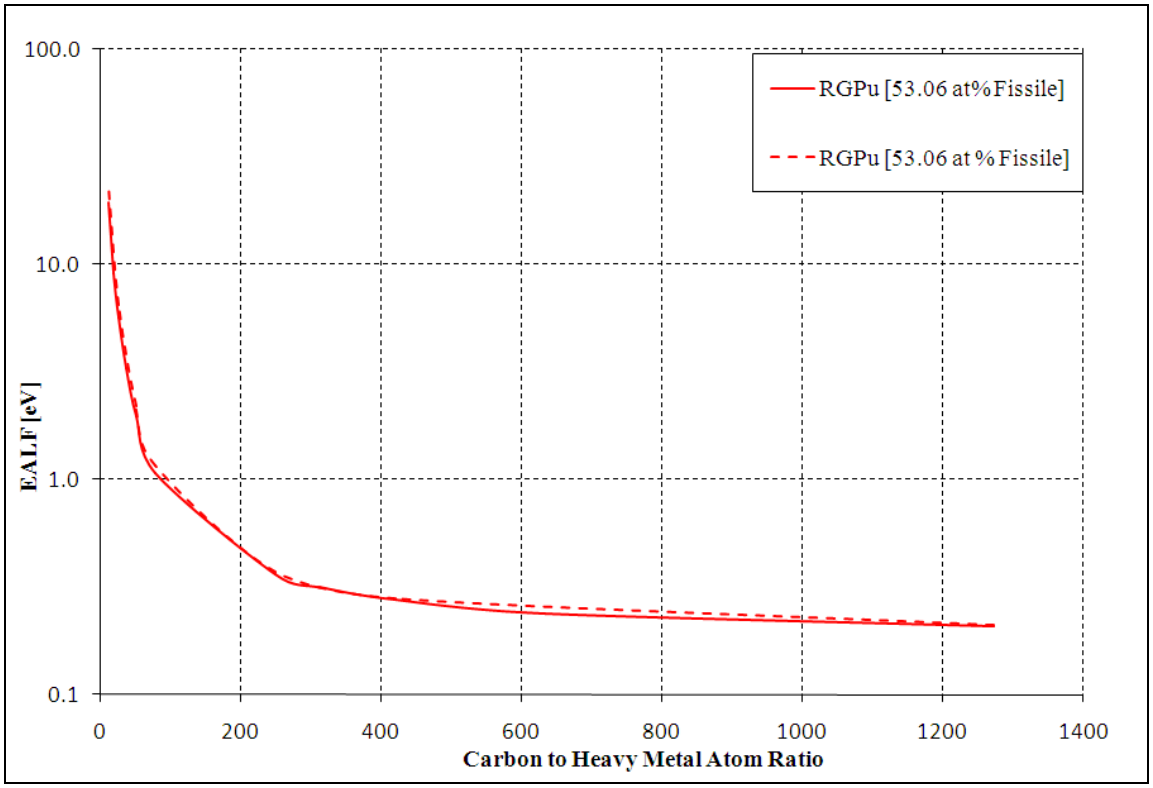

Fig 28. EALF for three and four fuel-ring VHTR fueled with RGPu for varying C/HM atom ratios.

The effect of C/HM on the flux in the RGPu-VHTR is more complex when compared to the effects observed in the LEU-VHTR systems. In Fig. 29, a distinct thermal peak and fast peak can be seen. This figure was produced for the RGPu-VHTR core with the C/HM atom ratio of 249 and k_{eff} of 1.19. For comparison, the flux shown in Fig. 30 is from the same VHTR but with a C/HM atom ratio of 36 and k_{eff} of 1.19. The flux shape in this reactor has no thermal peak in the compact. Figs. 29 and 30 show the energy-dependent flux for VHTR configuration that rest on opposite sides of the k_{eff} dip in Fig, 27. From the flux spectra shown in these figures, the k_{eff} anomaly shown as a dip in Fig. 27 can be explained as the transition from a thermal system to a system with a hard spectra.

When Fig. 30 (hard spectra) is compared to Fig. 25 (illustrating that low C/HM atom ratio LEU systems exhibit a thermal peak), the question of the thermal peak loss for RGPu systems with low C/HM atom ratio is raised. This loss can be explained by the nuclear characteristics of the RGPu vectors and reduction in moderation in the VHTRs with low C/HM atom ratios. This results in a decrease in the resonance escape probability as well as an increase in fission induced by fast neutrons.

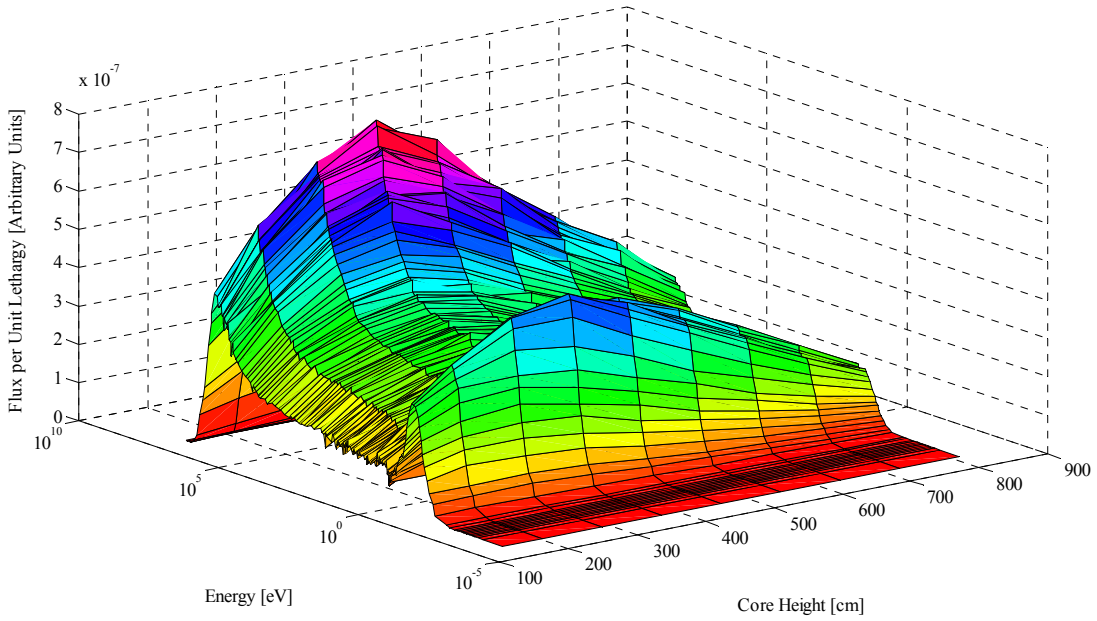

Note: Three fuel-ring RGPu (53.064 fissile atom fraction) VHTRs with a C/HM atom ratio of 249 in the inner most fuel-ring.

Fig 29. KENO V.a flux inside a compact for an RGPu-fueled system with a distinct thermal peak.

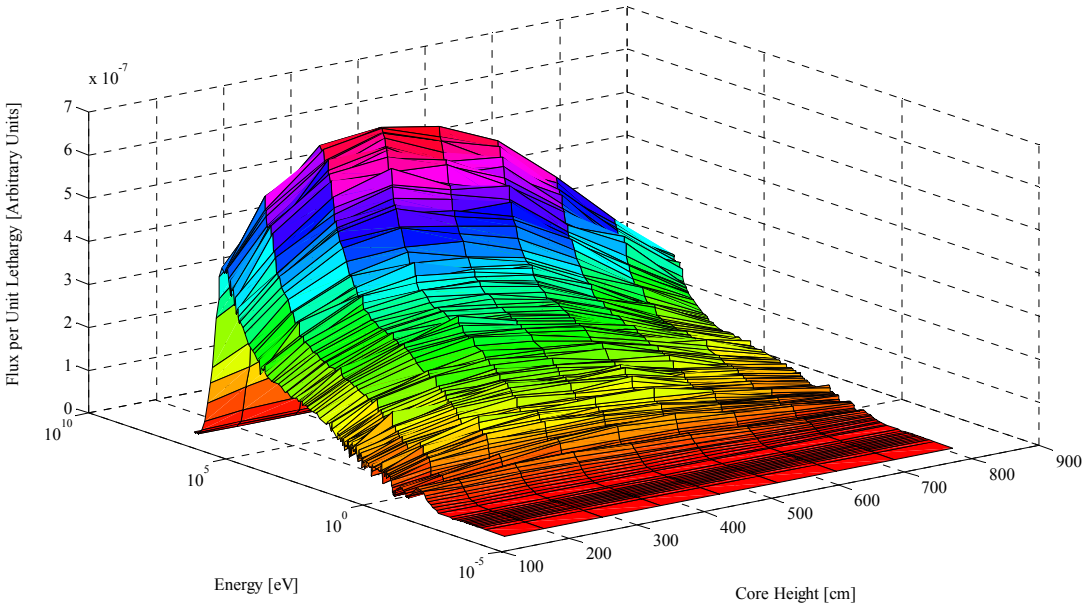

Note: Three fuel-ring RGPu (53.064 fissile atom fraction) VHTRs with a C/HM atom ratio of 36 in the inner most fuel-ring.

Fig 30. KENO V.a flux inside a compact for an RGPu-fueled system without a distinct thermal peak.

A series of varied C/HM reactor configurations were modeled for TRU-fueled VHTRs and the results of these models are given in Table XVII.

Table XVII. Reactor Physics Parameters for Three and Four Ring TRU-VHTR Configurations as a Function of C/HM Atom Ratio

Number of Rings	Fissile Atom Fraction	C/HM	k_{eff}	EALF [eV]	Avg. Neutron Fission Yield	MFP [cm]
3	53.064	1271.34	1.00	0.21	2.89	1.90
3	53.064	845.40	1.05	0.23	2.89	1.92
3	53.064	632.44	1.08	0.25	2.89	1.92
3	53.064	504.66	1.08	0.27	2.89	1.93
3	53.064	419.47	1.08	0.29	2.89	1.93
3	53.064	358.62	1.08	0.31	2.89	1.94
3	53.064	312.99	1.08	0.34	2.89	1.94
3	53.064	249.10	1.07	0.39	2.89	1.95
3	53.064	206.51	1.06	0.46	2.89	1.95
3	53.064	176.08	1.06	0.53	2.89	1.95
3	53.064	153.26	1.05	0.61	2.89	1.96
3	53.064	78.73	1.04	1.37	2.90	1.97
3	53.064	25.48	1.10	8.69	2.91	1.98
3	53.064	11.79	1.17	32.77	2.92	1.98
4	53.064	1271.34	1.04	0.21	2.89	1.82
4	53.064	845.40	1.09	0.23	2.89	1.83
4	53.064	632.44	1.11	0.25	2.89	1.84
4	53.064	504.66	1.11	0.27	2.89	1.85
4	53.064	419.47	1.11	0.30	2.89	1.85
4	53.064	249.10	1.09	0.41	2.89	1.87
4	53.064	176.08	1.08	0.55	2.89	1.88
4	53.064	78.73	1.05	1.51	2.90	1.89
4	53.064	25.48	1.11	10.05	2.91	1.91
4	53.064	11.79	1.18	38.38	2.92	1.91

Table XVII shows that, as the C/HM atom ratio decreases, the EALF and the MFP increases, much like VHTRs behave with RGPu fuel. Like the RGPu cases, k_{eff} does not

always increase as the C/HM atom ratio decreases. This attribute is illustrated in Fig. 31. In Fig. 31, it is apparent that in TRU-fueled cores, k_{eff} behave similarly to RGPu k_{eff} when C/HM is changed but at a lower k_{eff}. This behavior is expected, accounting for nuclear physics of TRU and reduction in moderation of low C/HM atom ratios similarly as discussed with RGPu-fueled VHTRs.

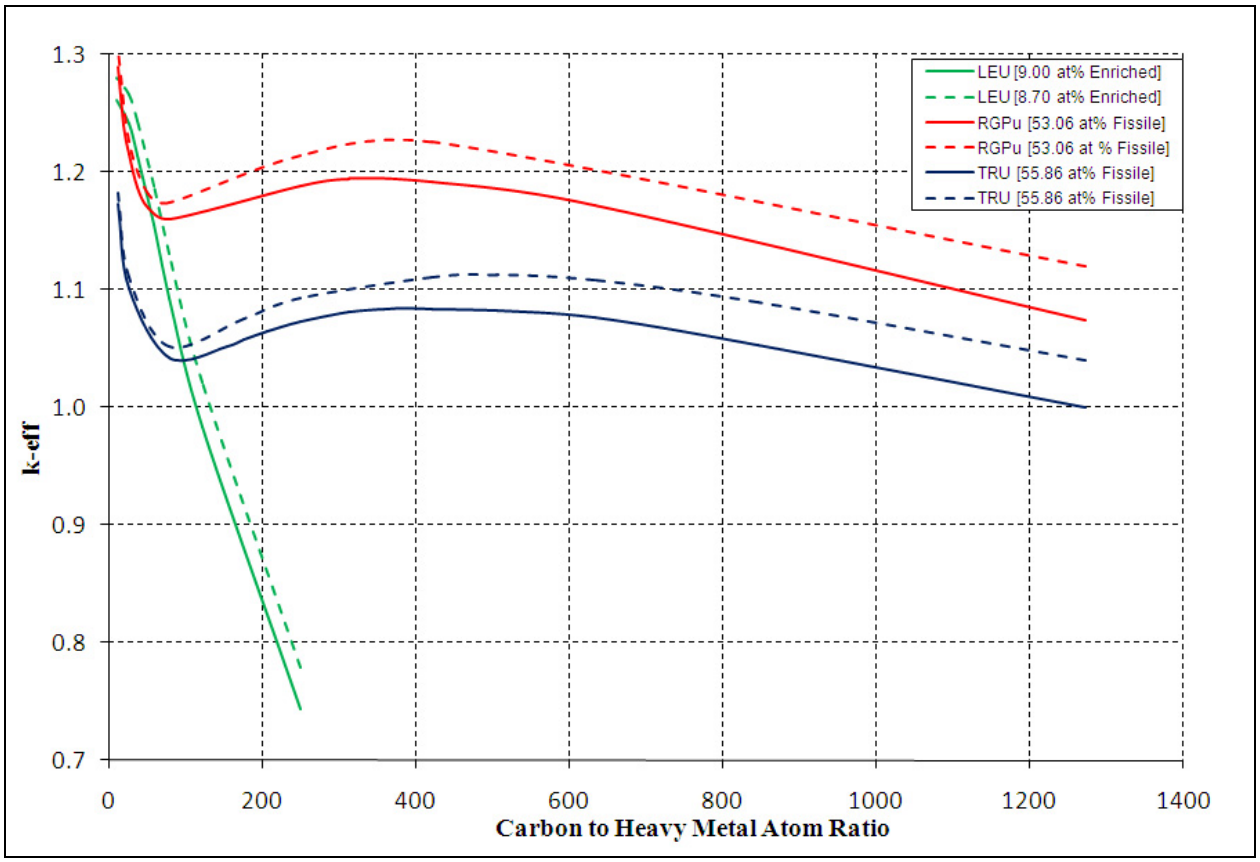

Note: Three and four fuel-ring VHTRs fueled by LEU, RGPu or TRU.

Fig 31. Keff for three and four fuel-ring VHTR fueled with TRU for varying C/HM atom ratios with LEU and RGPu cases shown for comparison.

The effect of C/HM on the flux in the TRU-fueled VHTRs is far more complex when compared to the effects on LEU systems and more complex than the RGPu-fueled

systems. In Fig. 32, a distinct thermal peak and fast peak can be seen in the flux. This figure was produced for the TRU-fueled core with the C/HM atom ratio of 505. For comparison, the flux shown in Fig. 33 is for a TRU-fueled VHTR with a C/HM atom ratio of 25. The flux shape in this reactor has no thermal peak present in the compact but when compared to Fig. 34 (the same core but with a C/HM ratio of 12) the fast peak has grown in magnitude and the slowing down region has been noticeably reduced in magnitude. This indicates that low C/HM TRU-fueled systems are capable of utilizing fast neutrons much better than higher ratio systems. The ability of these systems to utilize fast and slowing down neutrons could prove beneficial in allowing for long core lives.

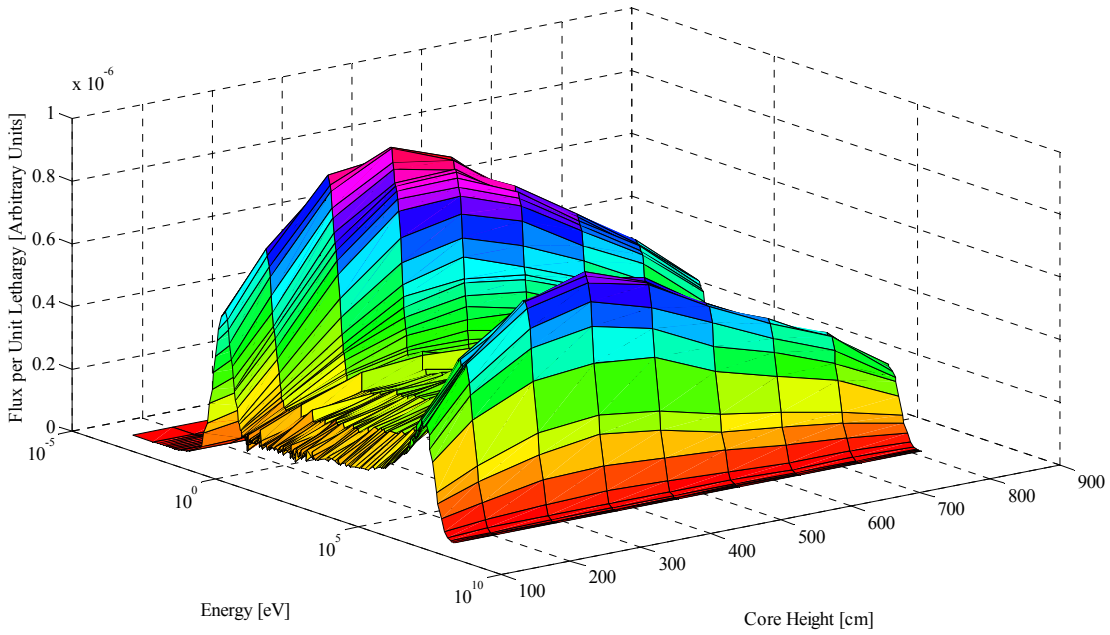

Note: Three fuel-ring TRU (55.86 fissile atom fraction) VHTR with a C/HM atom ratio of 505 in the inner most fuel-ring.

Fig 32. Flux calculated by KENO V.a inside a compact for a TRU-fueled system with a distinct thermal peak.

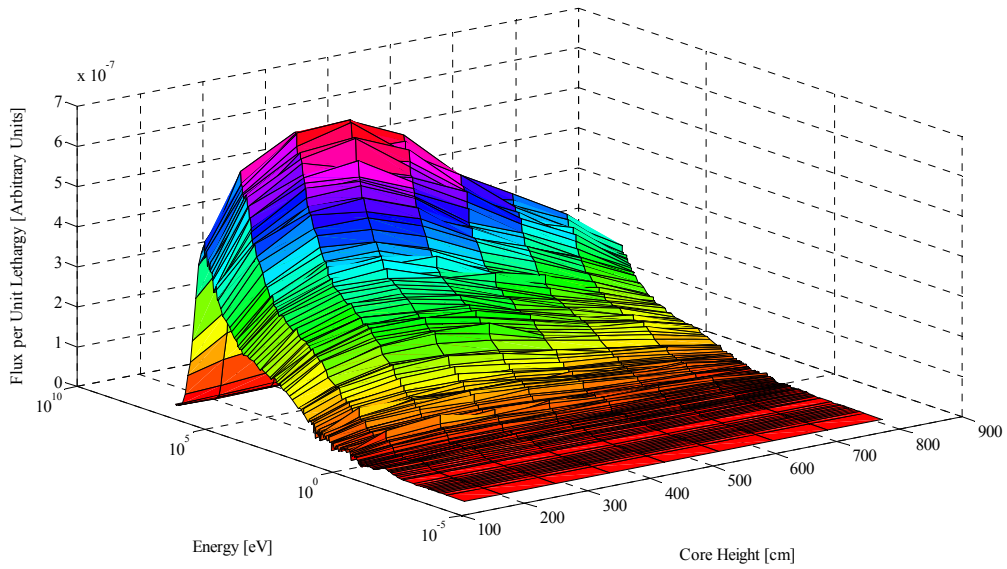

Note: Three fuel-ring TRU (55.86 fissile atom fraction) VHTR with a C/HM atom ratio of 25 in the inner most fuel-ring.

Fig 33. Flux calculated by KENO V.a inside a compact for a TRU-fueled system without a distinct thermal peak.

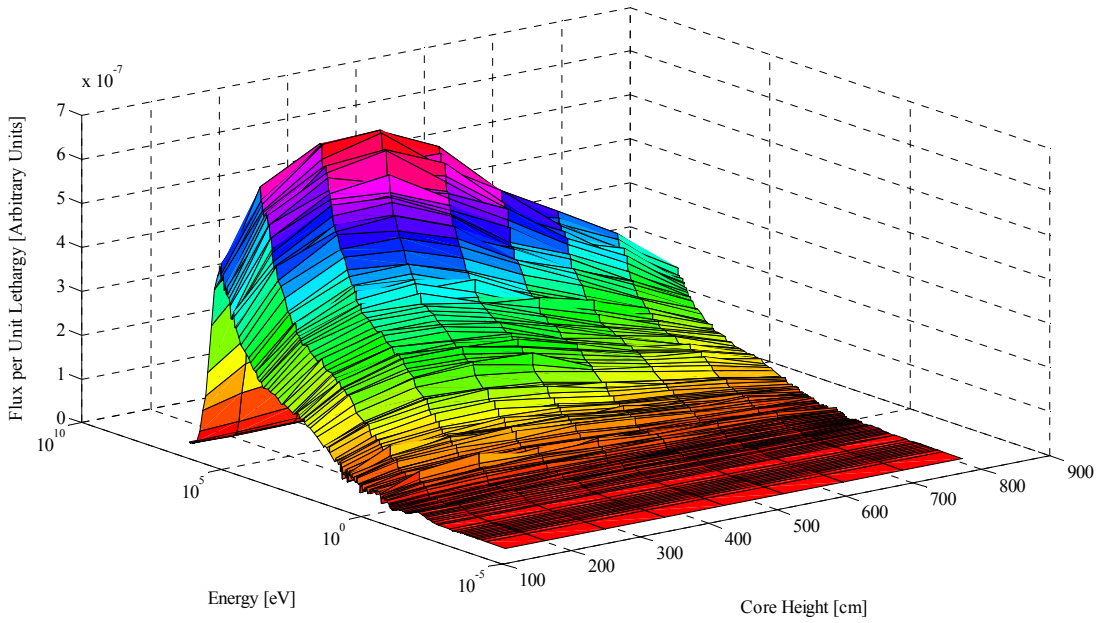

Note: three fuel-ring TRU (55.86 fissile atom fraction) VHTR with a C/HM atom ratio of 12 in the inner most fuel-ring.

Fig 34. KENO V.a flux inside a compact for a TRU-fueled system without a distinct thermal peak and higher magnitude fast flux peak.

Fig. 35 shows the energy dependent flux in four cases for TRU-fueled VHTRs. This figure demonstrates that, from fission energies to approximately energies of 1 keV, the flux for each core is about constant in shape but not in magnitude. After a C/HM ratio has dropped to approximately 100, the addition of more fuel significantly increases k_{eff} of the system such that compacts acts solely as a fast neutron source requiring neutrons to exit the compact before thermalization can occur. Such systems could prove more difficult to control and require further safety analysis.

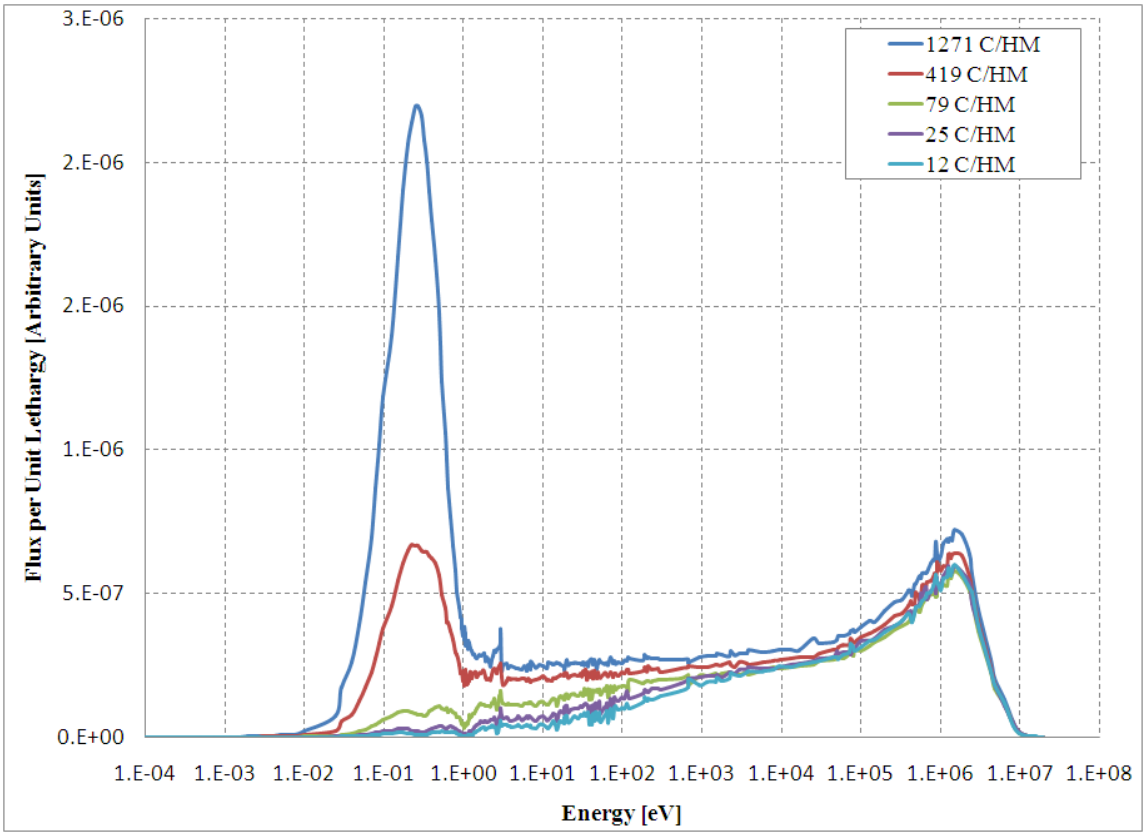

Fig 35. Flux calculated by KENO V.a inside a compact for a TRU-fueled systems.

IV.B Simplified Model

In this section the development of a simplified VHTR model is discussed. Due to limitations of T5-DEPL, a simplified version of the model used in the CSAS25 calculation was needed. Specifically, T5-DEPL, as available in SCALE 5.1 when released in 2006 could not deplete double heterogeneous materials. Due to the close working relationship between Texas A&M and the SCALE group at ORNL, SCALE 5.1 was patched to allow for the depletion of one double heterogeneous material. Another further simplification was needed to reduce computation time for each T5-DEPL case.

At each time-step in the a T5-DEPL model, new cross-sections have to be generated due changes in radionuclide concentrations. The radionuclide concentrations affect the energy-dependent flux shape and thus the reaction rates leading to depletion. In complex models, cross-section processing can take upwards of five hours for each time-step. With multiple time-steps, a T5-DEPL calculation could take two weeks to complete. To avoid such a scenario the calculation time was reduced by the removal of the temperature distribution. As stated in Section III, a temperature distribution was created by the addition of materials but with varying temperatures. Without these materials, there are fewer cross-sections that have to be processed at each time-step, requiring less computation time for a single T5-DEPL case.

The same physical geometry was used for both the simplified model and the detailed models used for BOL characterization in Section IV.B. To contrast the effects of having and not having a temperature distribution, four CSAS25 cases were evaluated with core configurations was identical to the four cases investigated in Section IV.B. The only difference between these cases is the active core average temperature (1250 K) used throughout the geometry. To clarify, each case was physically the same, had the same number of materials, but for each set of twin cases, one case had a temperature distribution while the other had a single temperature throughout the model. Results of

these cases are shown in Table XVIII and are compared to the results for the same core configurations as part of the investigations in Section IV.A.

Table XVIII. Results of Isothermal Core Average Temperature on CSAS25 Results

LEU Three Fuel-ring Configuration Enrichment=9% C/HM=36				
Temp. Dist.	**k_{eff}**	**EALF [eV]**	**Avg. Neutron Fission Yield**	**MFP [cm]**
No	1.220	0.238486	2.43878	1.91514
Yes	1.214	0.231661	2.4388	1.91412
LEU Three Fuel-ring Configuration Enrichment=9% C/HM=10				
Temp. Dist.	**k_{eff}**	**EALF [eV]**	**Avg. Neutron Fission Yield**	**MFP [cm]**
No	1.26575	0.571847	2.44185	1.94242
Yes	1.26076	0.566728	2.44188	1.94045
TRU Three Fuel-ring Configuration Fissile Atom Fraction=55.86% C/HM=505				
Temp. Dist.	**k_{eff}**	**EALF [eV]**	**Avg. Neutron Fission Yield**	**MFP [cm]**
No	1.08946	0.276809	2.89104	1.92939
Yes	1.08206	0.269326	2.89128	1.92861
TRU Three Fuel-ring Configuration Fissile Atom Fraction =9% C/HM=12				
Temp. Dist.	**k_{eff}**	**EALF [eV]**	**Avg. Neutron Fission Yield**	**MFP [cm]**
No	1.17548	33.33804	2.91770	1.98172
Yes	1.173	32.7658	2.91787	1.98003

The results summarized in Table XVIII show that systems have nearly identical reactor physics properties. These results led to the conclusion that the lack of a temperature distribution does not dramatically alter the VHTR modeling results, when accounted for by an accurate average temperature.

IV.C Safety of VHTRs

In this section, the reactivity coefficients were calculated to evaluate safety characteristics of TRU-fueled VHTRs. Four isothermal VHTR configurations were

modeled with CSAS25. These four cases are identical to the four isothermal cases used in Section IV.B but these cases used a core average temperature of 1350 K. Using these four cases, isothermal temperature coefficients were evaluated as:

$$\rho_n = \frac{k_{n+1} - k_n}{k_{n+1} \cdot k_n} \cdot \frac{1}{T_{n+1} - T_n}$$

Where:

ρ_n: Temperature coefficient between T_n and T_{n+1} $\left(\Delta k / k / K\right)$

T_n: Core Temperature at n^{th} measurement $\left(K\right)$

T_{n+1}: Core Temperature at $n+1^{th}$ measurement $\left(K\right)$

k_n: Effective Multiplication Factor at T_n

k_{n+1}: Effective Multiplication Factor at T_{n+1}

The results of these four cases are shown in Table XIX, with the corresponding temperature reactivity coefficient.

Table XIX. Isothermal Temperature Reactivity Coefficients

Case Summary	**Temperature Reactivity Coefficient** $\left(\Delta k / k / K\right)$
LEU C/HM=80 Enrichment=9%	-1.95E-05
LEU C/HM=30 Enrichment=9%	-3.43E-05
TRU C/HM=70	-5.07E-05
TRU C/HM=025	-7.16E-05

Calculated temperature reactivity coefficients for TRU-fueled VHTRs were found to be more negative then LEU-fueled VHTRs. In TRU systems, low C/HM systems have a temperature reactivity coefficient approximately the same as shown for high C/HM systems. In LEU systems, a low C/HM atom ratio core has approximately half the negative reactivity as a high C/HM system. This is caused by the harder spectrum which lowers the probability that a neutron will be absorbed in the broadened U-238 resonance capture cross-section.

IV.D Single-Batch Operation of theTRU-Fueled VHTRs

In this section, depletion cases were investigated for three fuel-ring VHTR cores based on characterizations of VHTR BOL operation domains in Section IV.A. Only TRU and LEU-fueled configurations were considered.. The TRU fuel composition used in this section differed in that fuel was not modeled as a dioxide (i.e., HM without oxygen in the fuel kernel). The effect of this simplification is negligibly small. As was demonstrated in prior sections, a 3D representation of the energy-dependent flux can be generated. The energy-dependent flux is generated at each time step in the T5-DEPL calculation. Fig. 36 shows the flux for a TRU-fueled VHTR with a low C/HM atom ratio of 11.

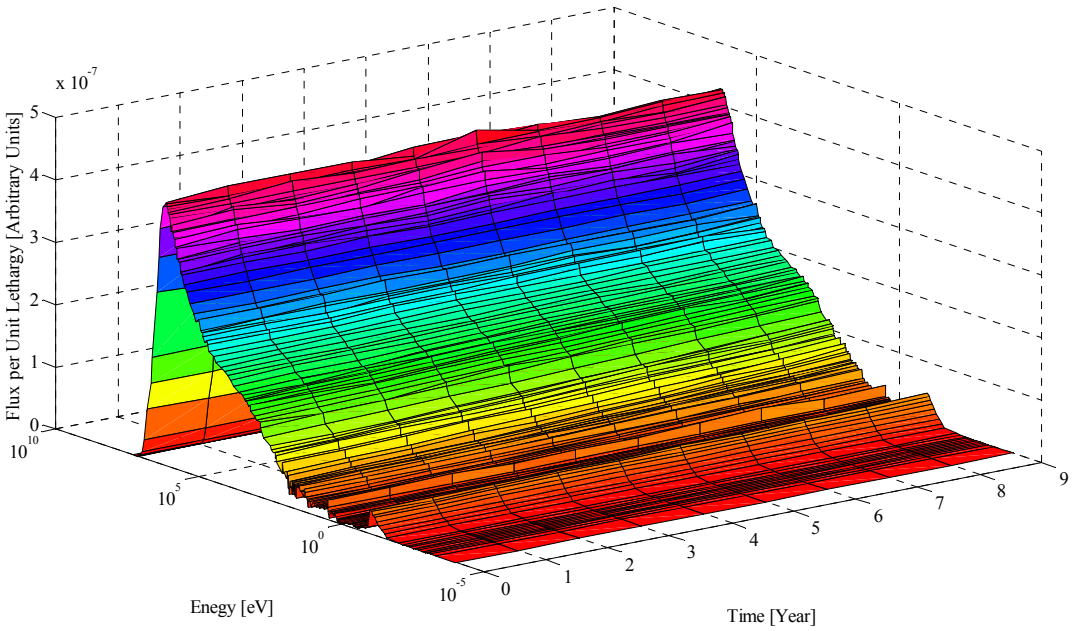

Fig 36. Energy-dependent flux during reactor operation for TRU-fueled VHTRs.

In Fig. 36, the energy dependent flux for the compact is shown for each time step of reactor operation. The hard spectrum encountered in the CSAS25 BOL calculations is still evident for core lives in T5-DEPL cases.

IV.D.1 Core Life-Time

Several TRU-fueled VHTR configurations have been analyzed to determine the effect of the C/HM atom ratio on the single-batch core lifetime. Fig. 37 illustrates the TRU-fueled VHTR operation in a single-batch mode.

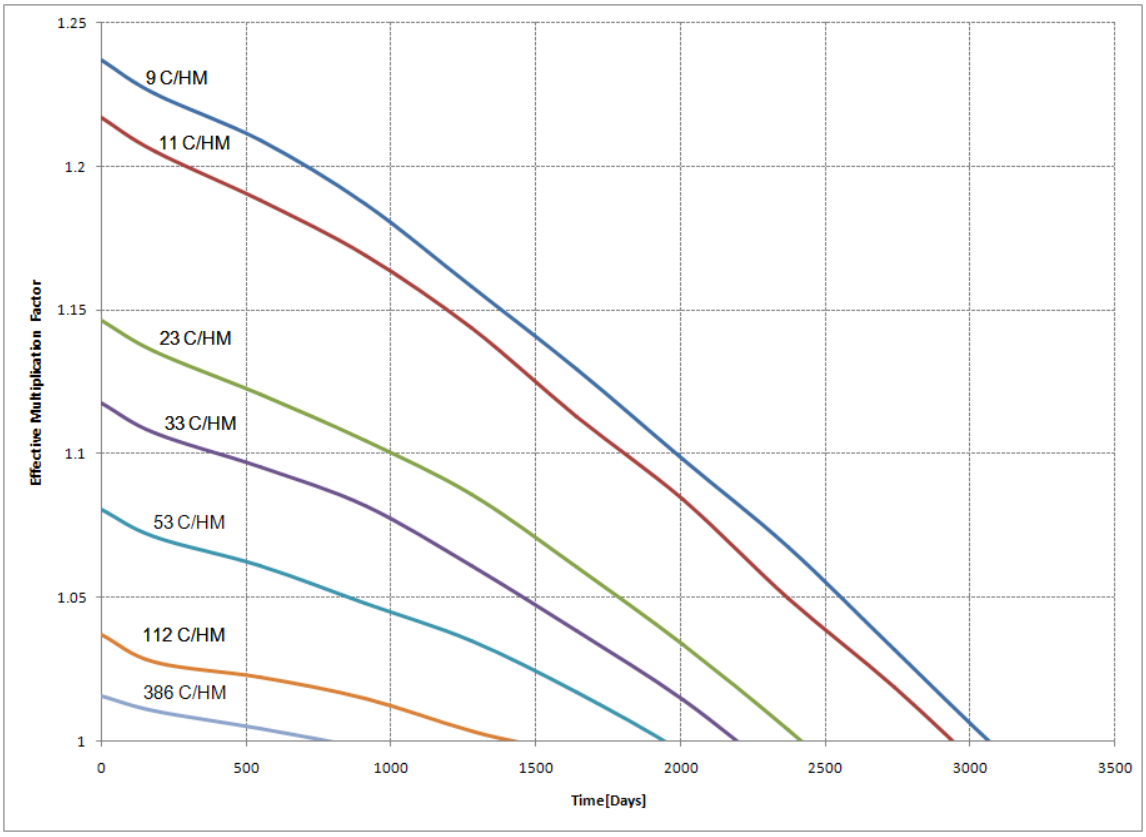

Fig 37. Single-batch operation of TRU-fueled VHTR configurations as a function of the C/HM atom ratio per compact.

The TRU-fueled VHTR configurations were considered assuming their operation at 103 MW/MTHM. Fig 37 illustrates that the core lifetime of 9 years is possible if attained fast fluence levels can be tolerated by TRISO particles. Furthermore, by simply adjusting the C/HM atom ratio inside a compact, the corresponding compact adjustment can extend core life-time from less than three years to nine years.

Several LEU-fueled VHTR configurations were analyzed to determine the effect of both enrichment and C/HM on core lifetime. Figs. 38 though 40 illustrate the results of these calculations. Fig. 38 shows results for 20% enriched LEU, Fig. 39 shows results for 15% enriched LEU, and finally Fig. 40 shows results for 10% enriched LEU.

The longest core life possible is shown to be approximately four years, less than half of what was calculated for TRU-fueled cores. Changes in C/HM atom ration inside the compact have little effect on core life-time. One important exception is that lower C/HM atom ratios have shorter core-lives than higher C/HM atom ratio LEU fuel cores. This is due to the lack in RGPu creation from the capture of thermalizing neutrons in U-238 resonances during beginning of core life.

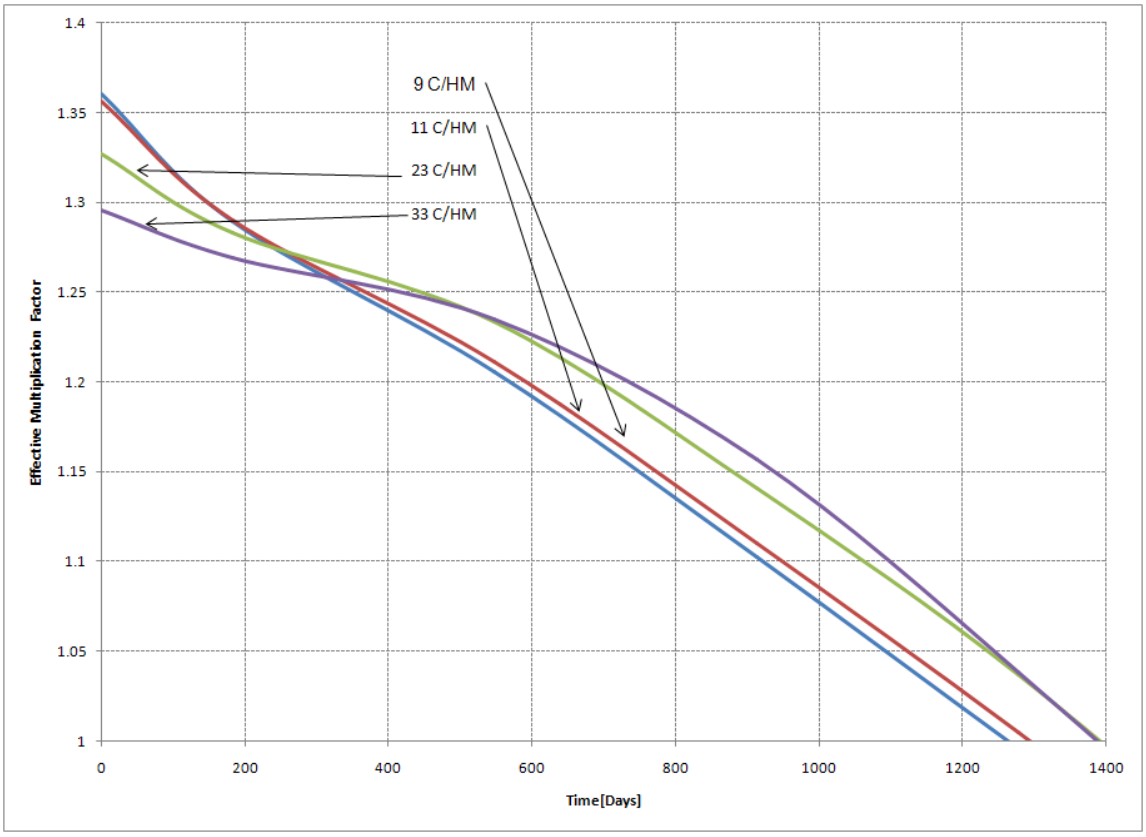

Fig 38. Single-batch operation of 20% LEU-fueled VHTR configurations as a function of the C/HM atom ratio per compact.

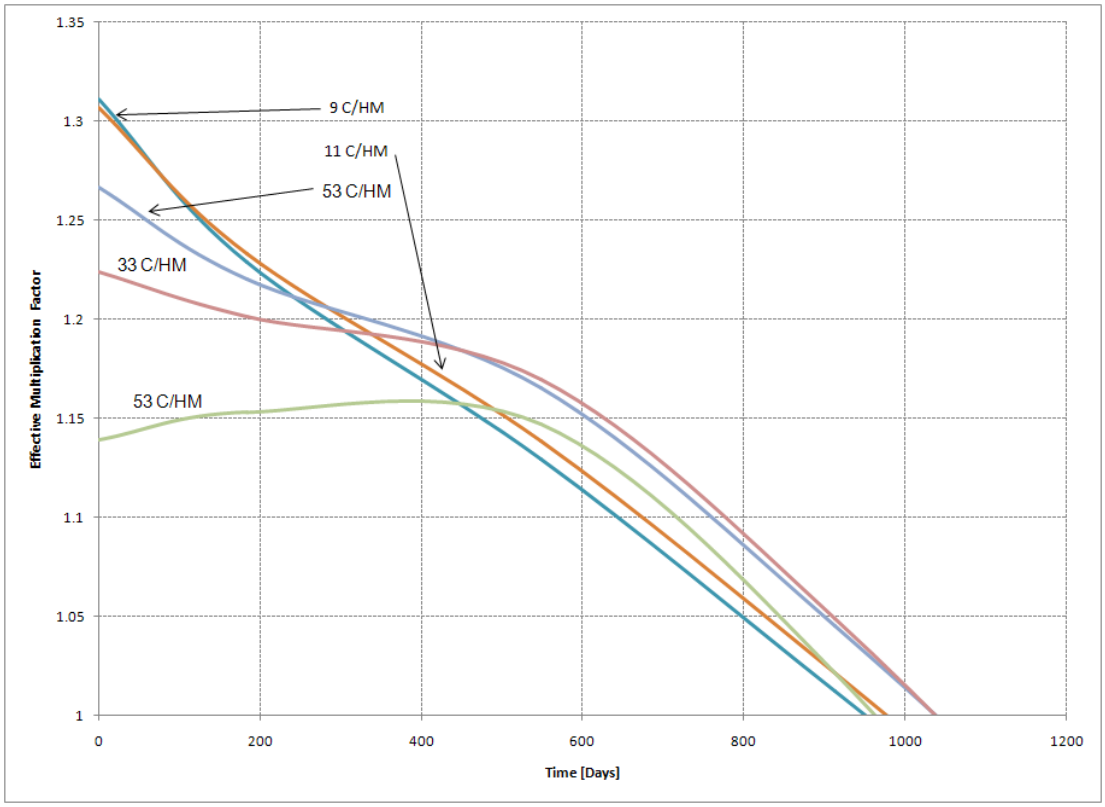

Fig 39. Single-batch operation of 15% LEU-fueled VHTR configurations as a function of the C/HM atom ratio per compact.

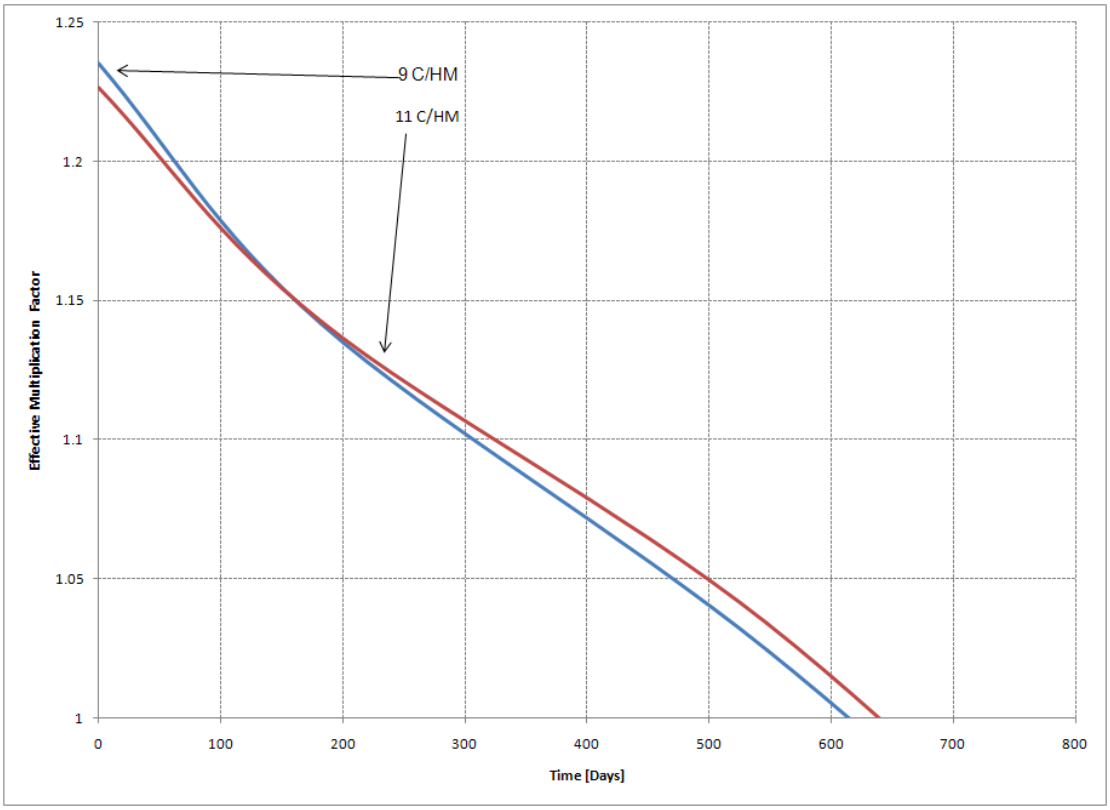

Fig 40. Single-batch operation of 10% LEU-fueled VHTR configurations as a function of the C/HM atom ratio per compact.

IV.D.2 Fast Fluence Levels in the TRU-Fueled VHTRs Operating in a Single-Batch Mode

Fast fluence, as discussed in Section II, is one of the most limiting factors in the operation of TRU VHTRs for extended lifetimes. Fig. 41 shows the fast fluence a TRISO particle would endure during core operation for cores shown to have the longest operation time.

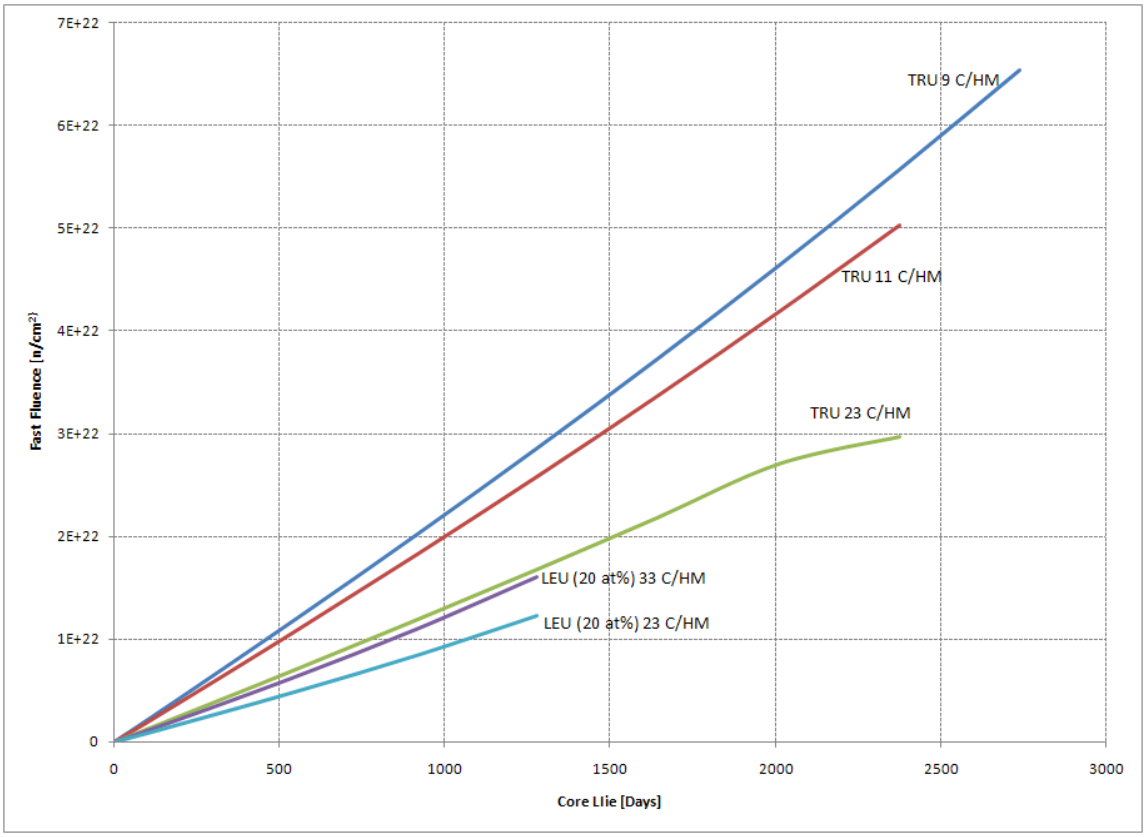

Fig 41. Fast fluence for longest operating VHTR configurations.

Fig. 41 shows that the highest fluence is approximately $7x10^{22}$ n/cm^2 whereas limiting fast fluence for TRISO particles is $5x10^{22}$ n/cm^2. With three orders of magnitude difference between safety limits and calculated fast fluences for the longest core lifetimes, the conclusion could be drawn TRU containing TRISO particles could be safely used for extended batch operation.

IV.D.3 TRU Destruction in VHTRs

As stated in Section I, TRU-fueled VHTRs have the possibility of TRU destruction. The calculated TRU destruction rates for TRU-fueled VHTR cores are shown in Table XX.

Table XX. TRU Destruction Rate

C/HM Atom Ratio	Core Life [years]	TRU Destruction [% $MTHM_{destroyed}$]
9	9	33.62%
11	8	29.86%
23	7	26.03%
33	6	22.26%
53	6	22.21%
112	5	18.44%
229	2	7.36%

As shown in Table XX, the destruction rate of TRU for VHTR is proportional to core life-time, where core life-time is dependent on the C/HM atom ratio in the compact. It is also important to note that low C/HM atom ratio cores contain more TRISO particles (i.e., more fuel) than do higher ratio cores.

IV.D.4 Radiotoxicity at EOL

When spent fuel is sent to the Yucca Mountain Geological Repository, SNF is going to be assessed on two factors. First, before a waste form can enter the subsurface environment, the waste package has to fall below a specific heat emission requirement. The heat a waste package emits is based on the configurations of the waste package and the activity and corresponding energy released from the waste. Since a waste package has not been designed to handle VHTR waste forms, SNF from a VHTR was judge on the energy being released per MTHM and energy being released per volume of HM that was originally placed in the reactor. Since the fuel originally placed in the VHTR was based on the average PWR TRU waste stream, calculations were performed on the longest lived core TRU VHTR configuration, so that the EOL actinide concentrations emitted the same energy per MTHM and energy per volume of HM exiting the reactor.

The second and most important criterion for SNF entering the geological repository is activity of the HLW. This is due to the dose requirements on personal working in the facility. Since dose levels are closely related to activities, activities of the actinide waste exiting the longest lived VHTR were analyzed based on the two metrics discussed for the energy emission requirements above. Fission products were not analyzed, under the assumption that they can be removed from a VHTR waste stream as was done with the PWR waste stream shown in Section III. Results of these calculations are shown in Table XXI.

Table XXI. TRU HLW from Longest VHTR Core Life

Time Required To Reach Same Energy Release per Fuel Volume	71 years
Time Required To Reach Same Energy Release per MTHM	164 years
Time Required To Reach Same activity per Fuel Volume	10 years
Time Required To Reach Same Energy Release per MTHM	23 years

V. CONCLUSIONS

A 3D whole-core model representing a power-size VHTR, accounting for both neutronics and thermal characteristics, was developed within the maximum limitations of the SCALE 5.1 code system. Both three and four fuel-ring annular core configurations were developed and analyzed. A 3D temperature distribution was developed based on conceivable operation conditions of a 600 MWth VHTR and was incorporated into the whole-core model for utilization in BOL CSAS25 calculations. The reactivity effects of the developed temperature distribution were compared to isothermal core distributions. Matlab and Perl scripts were developed and coupled with Excel files for rapid automated CSAS25 and T5-DEPL model generation, incorporating the developed 3D temperature distribution for use in CSAS25 parametric studies. Further, Matlab and Perl scripts were developed and utilized for efficient post-processing of simulation results obtained from SCALE 5.1 model outputs.

The effects on BOL criticality and fluxes were evaluated for varying U-235 enrichments and fissile nuclide fractions for RGPu three and four fuel-ring VHTR configurations. A strong dependence on BOL excess reactivity was found in both LEU and RGPu-fueled cores. The loss of a thermal peak in the neutron-energy spectra inside the compacts was shown for high fissile nuclide fractions in RGPu-fueled cores. A decrease in the magnitude of the thermal peak was shown for LEU-fueled systems. Excess reactivity at BOL was increased in LEU, RGPu, and TRU-fueled four fuel-ring configurations when compared to three fuel-ring configurations with identical fuel loadings. No measurable effects were found between three and four fuel-ring configurations with respect to the neutron energy spectra.

The effects on BOL criticality and fluxes were evaluated for varying C-to-HM atom ratios inside the compact. Ratios were changed by varying the packing fraction of TRISO particles inside the compact. A strong dependence on BOL excess reactivity was found in both LEU, RGPu and TRU-fueled cores. Increases in excess reactivity was

found for all three fuel types when the C/HM atom ratio was lowered, though in TRU and RGPu cases, the excess reactivity dropped for an intermediate range of C/HM atom ratios as a result of the systems moving from a thermal operation to systems with a hard neutron spectra. Neutron energy spectra were found to be capable of shifting by C/HM atom ratio adjustments in all three fuel types.

The effect of having a temperature distribution to BOL excess reactivity calculation was evaluated by the comparison of identical models that had hard or thermal spectras for TRU and LEU-fueled cores, for cases with and without a temperature distribution. Results showed that, when appropriate average core temperatures were used, excess reactivity changes were negligible.

Isothermal temperature reactivity coefficients were found to be adequately negative for LEU and TRU-fueled VHTRs. Additionally, TRU-fueled VHTRs were found to be safer due to a larger negative magnitude isothermal temperature reactivity coefficient then LEU-fueled VHTRs. Fast fluences were calculated for TRU and LEU-fueled cores and were found to be satisfactory in all sustainable core lives.

LEU and TRU-fueled VHTR models core operation lives were evaluated via the depletion of fuel within the double heterogeneous compacts via a non-public distributed version of TRITON through the T5-DEPL sequence. Nine year core-lives were found possible for single batched TRU-fueled cores without intermediate refueling during continuous operation conditions. Four year core-lives were possible for single batched LEU-fueled cores without intermediate refueling during continuous operation conditions.

Heavy metal destruction rates of approximately thirty-three percent were found possible for TRU-fueled VHTRs operating for extended core-lives and low C/HM atom ratios. Radiotixicity of exiting heavy metal waste streams of extended core lives was found to require minimal cooling time when compared to intial heavy metal fuel loading.

The characterization of TRU-fueled VTHRs resulting from the research showed promising results for future work. Future work should include but not be limited to:

- Coupled thermodynamic and neutronic codes for detailed investigation in relation to power distribution through core-life.
- Parametric studies of multiple fuel loading, fuel types, and fuel configurations for utilization of neutron energy spectra axial and radial distributions.
- Cross-section sensitivity studies related to composition changes during core-life.
- Quantification of uncertainty effects related to nuclear data and design parameters.
- Cost feasibility of long-life TRU-fueled VHTRs.

TRU-fueled VHTRs show promise in regards to protecting the environment while addressing the needs for cleaner and, more importantly, sustainable safe energy. This is possible due to the inherent safety, low environmental impact, and proliferation resistance of very high temperature reactors.

REFERENCES

1. N. CERULLO, D. BUFALINO, G. FORASASSI, G. LOMONACO, P. ROCCHI and V. ROMANELLO, "The Capabilities of HTRs to Burn Actinides and to Optimize Plutonium Exploitation," Proc. of ICONE12 April 25-29 2004, ICONE, Arlington, Virginia (2004).

2. L. BAETSLE, "Application of Partitioning/Transmutation of Radioactive in Radioactive Waste Management," Nuclear Research Centre of Belgium, Mol, Belgium (2001).

3. 107TH CONGRESS, "The Atomic Energy Act of 1982, As Amended," Nuclear Regulatory Legislation; 1st Session, Office of the General Counsel. US Nuclear Regulatory Commission, United States of America (2002).

4. NUCLEAR ENERGY RESEARCH ADVISORY COMMITTEE and THE GENERATION IV INTERNATIONAL FORUM, "Generation IV Roadmap Fuel Cycle Assessment Report," United States of America (2002).

5. M. RICHARD, "Yucca Mountain Program Overview," Department of Energy, Office of Civilian Radioactive Waste Management, United States of America, (2007).

6. DEPARTMENT OF ENERGY, "Report to Congress: Spent Nuclear Fuel Recycling Program Plan," United States of America (2006).

7. NUCLEAR ENERGY AGENCY, "Fuels and Materials for Transmutation: A Status Report," NEA No. 5419, France (2005).

8. T. TAIWO and R. HILL, "Summary of Generation-IV Transmutation Impacts," Nuclear Energy Division, Argonne National Laboratory (2005).

9. NUCLEAR ENERGY AGENCY, "Accelerator-driven Systems (ADS) and Fast Reactors (FR) in Advanced Nuclear Fuel Cycles," Nuclear Development-NEA, France (2002).

10. P. V. TSVETKOV, "Utilization of Minor Actinides as a Fuel Component for Ultra-Long Life VHTR Configurations: Designs, Advantages and Limitations: First Year Report," Texas A&M University, College Station, Texas (2006).

11. IAEA, "Safety and Environmental Aspects of Partitioning and Transmutation of Actinides and Fission Products," Proc. of a Technical Meeting, 29 November-2 December 1993, IAEA, Vienna, Austria (1995).

12. OECD Nuclear Energy Agency, "Partitioning and Transmutation of Minor Actinides and Fission Products". NEA, France (2006).

13. E. COLLINS, D. BENKER, L. FELKER, R. TAYLOR, G. DEL CUL, B. SPENCER, W. BOND, and D. CAMPBELL, "Development of the UREX+3 Flowsheet-An Advanced Separations Process for Spent Fuel Processing," ORNL. ANS Winter Meeting (2005).

14. DEPARTMENT OF ENERGY, "Generation IV Nuclear Energy Systems Ten Year Program Plan Volume I", March 27, 2005, Office of Nuclear Energy, Science, and Technology, United States of America (2005).

15. G. RIMPAULT, "Preliminary Design Studies of an Experimental Accelerator-Driven System," ADOPT, PDS-XADS United States of America (2003).

16. E. ELBARADEI, "Nuclear Power and Sustainable Development", IAEA (2006).

17. OFFICE OF NUCLEAR ENERGY, SCIENCE, AND TECHNOLOGY, "The US Generation IV Implementation Strategy", 03-GA50439-06, United States of America (2003).

18. P. MACDONALD, "Advanced Reactor, Fuel Cycle, and Energy Products Workshop for Universities," Department of Energy, United States of America (2004).

19. D. HANSON, "Screening Tests for Selection of VHTR Advanced Fuel," General Atomics, San Diego (2003).

20. T. TAIWO, T. KIM, W. YANG, and H. KHALIL, "Evaluation of High Temperature Gas-Cooled Reactor Physics Experiments as VHTR Benchmark Problems," Argonne National Laboratory (2005).

21. T. KIV, T. TAIWO, R. HILL, and W. YANG, "A Feasibility Study of Reactor-Based Deep-Burn Concepts," Nuclear Energy Division, Argonne National Laboratory (2005).

22. G. BRUNA, R. LABELLA, C. TRAKAS, A. BAXTER, C. RODRIGUES, and F. VENNERI, "Uncertainty Analysis and Optimization Studies on the Deep-Burner – Modular Helium Reactor for Actinide Incineration," PHYSOR, ANS, United States of America (2004).

23. D. E. AMES II, "Master of Science Thesis: Configuration Adjustment Potential of the Very High Temperature Reactor Prismatic Cores with Advanced Actinide Fuels," Texas A&M University, College Station, Texas (2006).

24. LOS ALAMOS NATIONAL LABORATORY, “Advanced Fuel Cycle Initiative, National Program,” United States of America (2003).

25. DEPARTMENT OF ENERGY, “AFCI Program Plan,” United States of America (2004).

26. DEPARTMENT OF ENERGY, “The Global Nuclear Energy Partnership”, United States of America (2006).

27. OAKRIDGE NATINAL LABORATORY, “SCALE: A Modular Code System for Performing Standardized Computer Analyses for Licensing Evaluations,” ORNL/TM-2005/39, Version 5.1. Available from Radiation Safety Information Computational Center at Oak Ridge National Laboratory as CCC-732 (2006).

28. IAEA, “Evaluation of HTGR Performance: Benchmark Analysis Related to Initial Testing of the HTTR and HTR-10,” Nuclear Power Technology Development Section, Vienna, Austria (2003).

VITA

Tom Goslee Lewis, III received his Bachelor of Science degree in nuclear engineering at Texas A&M University in 2005. He entered the Master of Science program in the nuclear engineering program at Texas A&M University in September 2005.

Mr. Lewis may be reached at 154 Squires Bend, Stafford, TX 77477. His email is tglewis3@gmail.com.